Title

Magnetic reconnection, helicity dynamics, and hyper-diffusion

Journal

Astrophysical Journal, 757(2)

ISSN

0004-637X

Authors

Guo, ZB
Diamond, PH
Wang, XG

Publication Date

2012-10-01

DOI

10.1088/0004-637X/757/2/173

Peer reviewed

The Astrophysical Journal, 757:173 (15pp), 2012 October 1 doi:10.1088/0004-637X/757/2/173

MAGNETIC RECONNECTION, HELICITY DYNAMICS, AND HYPER-DIFFUSION

Z. B. Guo[1], P. H. Diamond[2,3], and X. G. Wang[1]
[1] Physics Department and State Key Laboratory of Nuclear Physics and Technology, Peking University, Beijing, China; guozhipku@gmail.com
[2] WCI Center for Fusion Theory, National Fusion Research Institute, Daejeon 305-806, Republic of Korea
[3] Center for Astrophysics and Space Sciences and CMTFO and Department of Physics, University of California at San Diego, La Jolla, CA 92093-0424, USA
Received 2011 December 10; accepted 2012 August 16; published 2012 September 14

ABSTRACT

We examine the influence of noise and Alfvén wave turbulence on magnetic reconnection in a reduced magnetohydrodynamics model. We focus on the dynamics of magnetic helicity density. Helicity conservation is then used to calculate the global reconnection rate in terms of the helicity density flux. Two specific scenarios are explored—noisy reconnection and Alfvén wave turbulent reconnection. For noisy reconnection, the current sheet is assumed to sit in a noisy state, marginal to plasmoid formation instability. The scaling of the reconnection rate in the presence of noise is proportional to $(S_0^2/V_AL^2)^{1/11}$, where S_0^2/V_AL^2 is the relative amplitude of the noise. We obtain this prediction using a symmetry analysis of the helicity density flux. For Alfvén wave turbulent reconnection, a mean field closure scheme is applied. A reconnection rate proportional to $(\langle\tilde{B}^2\rangle/\langle B\rangle^2)^{1/8}$ is obtained, where $\langle\tilde{B}^2\rangle/\langle B\rangle^2$ and $\langle B\rangle$ are the relative energy of Alfvén wave turbulence and the reconnecting field. The constraint on reconnection rate enforced mean-square magnetic potential conservation is reexamined. A critical magnetic Reynolds number $R_{m,c}$ is identified. For $R_m \gg R_{m,c}$, the reconnection rate becomes independent of Spitzer resistivity and thus can be higher than the Sweet–Parker model prediction. Both cases exhibit a weak dependence of the reconnection rate on the amplitude of the turbulence. Therefore, even noise or weak turbulence can trigger fast reconnection if the system is marginally stable. The important distinction between turbulent reconnection and turbulent dissipation of magnetic energy is also discussed.

Key words: magnetic fields – magnetic reconnection – magnetohydrodynamics (MHD) – turbulence

Online-only material: color figures

1. INTRODUCTION

Magnetic reconnection is a ubiquitous phenomenon in laboratory, heliophysical, and astrophysical plasmas (e.g., Parker 1979; Biskamp 2000; Priest & Forbes 2000). In laboratory plasmas, examples are "sawteeth," disruptions (Kadomtsev 1975; Diamond et al. 1984), and reverse-field pinch relaxation (Taylor 1974). In the magnetosphere, magnetic energy carried by the solar wind is released into the inner magnetosphere through dayside and nightside reconnection processes. In solar physics, there are intensive studies of phenomena such as solar flares, the solar dynamo, and coronal mass ejections (Priest & Forbes 2000). Magnetic reconnection is also an element in many astrophysical phenomena such as dynamos and star formation in the interstellar medium, angular momentum transport in accretion disks, and γ-ray bursts in compact objects (Zweibel & Yamada 2009). Associated with the dissipation of magnetic energy and alteration of magnetic field topology, phenomena linked to magnetic reconnection can be classified into two groups: sudden magnetic energy release (e.g., flares) and the self-organization of magnetic configurations (e.g., relaxation and dynamos).

The basic paradigm of magnetic reconnection is the Sweet–Parker (SP; Sweet 1958; Parker 1957) model. In the model, the current sheet has a "Y"-point-type geometry, and this strongly anisotropic structure greatly reduces the reconnection rate. The resulting reconnection rate is $V_{\rm in} = V_A/\sqrt{S}$. Here V_A is the Alfvén velocity associated with the reconnecting field, $S = V_AL/\eta$ is the Lundquist number, L is the macroscale of the system, and η is the Spitzer resistivity. In many astrophysical environments, S is huge, e.g., in the solar corona $S \sim 10^{13}$, and in interstellar media $S \sim 10^{20}$ (Ji & Daughton 2011). The reconnection rate given by the SP model is then far too slow to explain rapid transient phenomena in such high Lundquist number plasmas. For example, the timescale of the solar flare is minutes to hours, while the magnetic diffusion time on the scale of a typical solar flare of 10^6 years leads to a magnetic reconnection timescale of years. Many other applications also require a fast reconnection rate. These strongly motivate studies of fast magnetic reconnection mechanisms.

Given the physical simplicity and the dependence of the SP model on only mass, momentum, and energy conservation, many extensions of that model have been proposed. The first attempt was to include plasma compressibility (Petschek 1964). By invoking slow shock structure, the current sheet acquires an "X" point geometry, and a reconnection rate of $V_A/\ln S$ is predicted, fast enough to explain observations. Subsequent numerical simulations, however, showed that for a spatially uniform resistivity, the reconnection configuration preferred the SP model prediction, not the Petschek, particularly for high Lundquist number plasmas (Biskamp 1986). Theoretical studies (Kulsrud 2000) also showed that the Petschek model was inconsistent, due to the fact that reconnection could not produce enough transverse magnetic field to support the shock structure (Kulsrud 2000). By assuming a spatially inhomogeneous anomalous resistivity, investigations showed that an "X"-point current sheet was formed and a Petschek-like fast reconnection rate was then obtained (Biskamp & Schwarz 2001; Kulsrud 2001, 2005; Uzdensky 2003). This result can be understood as follows: if anomalous resistivity has a maximum at the X-point and decreases away along the current sheet, a large reconnection angle can be formed and thus the reconnection rate increases with the wide open exit for the reconnected flux (Zweibel & Yamada 2009). This prediction has been observed in certain

numerical simulations (Biskamp 1986; Malyshkin et al. 2005) but is yet not verified experimentally. Another line of development is to apply collisionless reconnection models by including different kinetic effects at smaller scales, such as Hall effects (Wang et al. 1996; Shay et al. 2001; Birn et al. 2001) and anomalous resistivity (Sagdeev & Galeev 1969; Papadopoulos 1977). Further discussions on the effects are given in Section 4.

On the other hand, plasmoid structures in thin current sheets formed during the reconnection process are observed in resistive MHD simulations in the high Lundquist number regime (Samtaney et al. 2009; Huang & Bhattacharjee 2010). This is thought to be another viable mechanism to reach a fast reconnection rate (Shibata & Tanuma 2001; Drake et al. 2003, 2006). Though the physical explanation of the role of the plasmoid in magnetic reconnection is not clear yet, this scenario reveals certain interesting properties such as the effect of criticality and the appearance of micro-structures (plasmoids). The basic idea in plasmoid reconnection is to see the dissipation regime as an ensemble of N_p small-scale current sheets. For each current sheet, one has $L_p \sim L/N_p$ and $\Delta_p \sim \Delta/\sqrt{N_p}$, where L_p, Δ_p are the length and width of each microscopic current sheet, L, Δ are the length and width of the macroscopic diffusion region, and N_p is the number of plasmoids (Daughton et al. 2009). Then, one can obtain the global reconnection rate $V_{\rm in} \sim V_{\rm SP}\sqrt{N_p}$, where $V_{\rm SP}$ is the SP reconnection rate. Theoretical studies on plasmoid reconnection in the linear regime predicted that plasmoids were generated by tearing-like instability (Loureiro et al. 2007). This type of reconnection is then inherently time dependent and impulsive and bears some similarities to transport phenomena near the marginal state.

Magnetic reconnection in a pre-existing and externally excited turbulent plasma environment, usually called turbulent reconnection, is an outstanding problem, since turbulence pervades in astro- and lab-systems (Armstrong et al. 1995; Diamond et al. 2005). Though there exist evidences (Diamond et al. 1984; Matthaeus & Lamkin 1985, 1986; Lazarian & Vishniac 1999; Retinò et al. 2007; Kowal et al. 2009) that turbulence can play an important role in reconnection, the physical mechanism of turbulent reconnection is still not well understood (Kim & Diamond 2001; Zweibel & Yamada 2009). Another important motivation to study turbulent reconnection is its connection with the magnetic dynamo problem, since an efficient generation rate of large-scale magnetic fields inevitably requires fast rearrangement of magnetic field topology (reconnection). The turbulent reconnection process studied in this work occurs due to the spatial mixing of the reconnecting field by the turbulent velocity and magnetic fields. It is a pure fluid dynamic process and, in principle, is different from that in the kinetic regime where wave–particle interaction is essential. We should first clarify the following questions for turbulent reconnection: (1) What is the role of turbulence? (2) What is the difference between turbulent reconnection and turbulent dissipation? (3) What are the conditions for turbulent reconnection to occur? (4) What is the mechanism for breaking the mean field freezing-in condition?

In reply to question (1), the turbulence acts as a "trigger" for turbulent magnetic reconnection. We can see this through the two main properties of our turbulent reconnection models: (a) the reconnection rate weakly depends on the amplitude of turbulence, and (b) the reconnection process exhibits critical behavior. For question (2), in turbulent dissipation or cascade, the relaxation is driven by the nonlinear interaction of fluctuating fields, and the magnetic energy dissipation rate is linearly

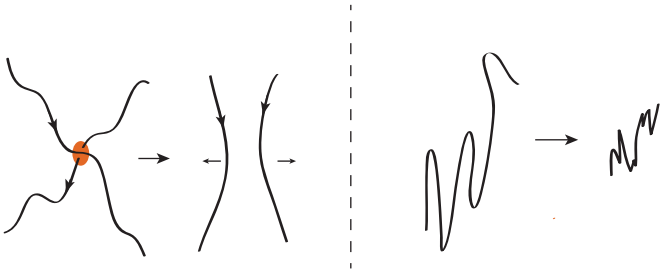

Figure 1. Distinction between turbulent reconnection (left) and turbulent scrambling (right).

(A color version of this figure is available in the online journal.)

proportional to the injected power. In turbulent reconnection, turbulence produces mean field dissipation. The nonlinear interaction occurs between reconnecting and fluctuating fields and is non-local in scale. Since noise is only a trigger for the relaxation, the dissipation rate should depend only weakly on the amplitude of the noise. This property will be demonstrated in the scaling analysis of the reconnection rate in our following calculations. For question (3), turbulent reconnection occurs only in a weakly turbulent system, where $\langle \tilde{B}^2 \rangle \ll \langle B \rangle^2$. Once reconnection occurs, the system departs from the initial state and evolves to a new reconnected state through the dynamical evolution of large-scale fields. When $\langle \tilde{B}^2 \rangle \gg \langle B \rangle^2$, the topology of mean magnetic field lines becomes ambiguous. It is hard to trace them, and then the main magnetic energy dissipation mechanism is turbulent wind-up, mixing and scrambling of the large-scale field, but not reconnection (Figure 1). Formulating a reconnection problem requires an identifiable field with at least a component that changes sign. Question (4) is about the origin of irreversibility in turbulent reconnection. What happens in turbulent reconnection is the change of mean magnetic field topology, so breaking of the freezing-in law refers to the mean magnetic field $\langle B \rangle$. From our two specific models discussed later in this work, we will show that the irreversibility in turbulent reconnection originates from the turbulent dissipation of the mean field $\langle B \rangle$ by fluctuation field $\tilde{B}$. The basic physical process is that the turbulent field is excited by external forcing or by the reconnecting field's dynamics. Then the turbulent energy cascades to small scales through nonlinear interaction and is dissipated by viscosity and resistivity. More explicitly, the turbulent dissipation can be equivalently described as an effective hyper-diffusion process by using a turbulence closure model.

In this work, we study the problem of turbulent reconnection from the perspective of dynamical evolution of magnetic helicity density, which describes the local topology of magnetic field, since the topological change of magnetic field lines is well described in that framework. In fact, magnetic reconnection can be regarded as a process of conversion between different forms of magnetic helicity, while the total magnetic helicity is conserved in the process (Woltjer 1958; Taylor 1974; Wright & Berger 1989). An essential feature of this relaxation process is that the profile of the current sheet tends to broaden, to the lowest order, corresponding to the diffusion of current density (hyper-diffusion) to approach $\nabla J_\parallel = 0$, where $J_\parallel$ is the current density along mean magnetic field. From the perspective of helicity dynamics, we also know that turbulent helicity density flux plays a crucial role in reconnection. Thus, we can expect that there exist some close relations between helicity density flux and hyper-diffusion. There are already several works (Boozer 1986; Bhattacharjee & Hameiri 1986; Diamond & Malkov 2003)

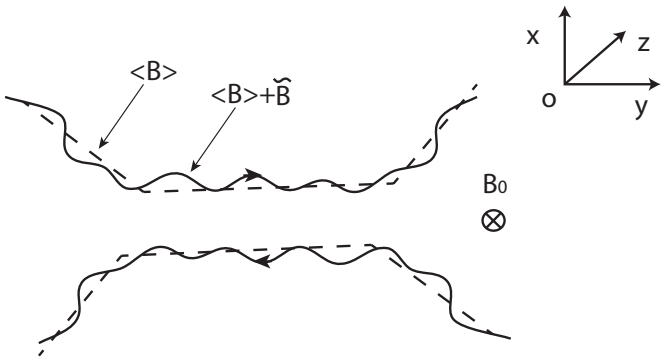

Figure 2. Turbulent reconnection configuration: B_0 is a strong guiding field in $\hat{z}$, $\langle B\rangle$ is the reconnecting field in $\hat{y}$, and $\tilde{B}$ is the fluctuation field.

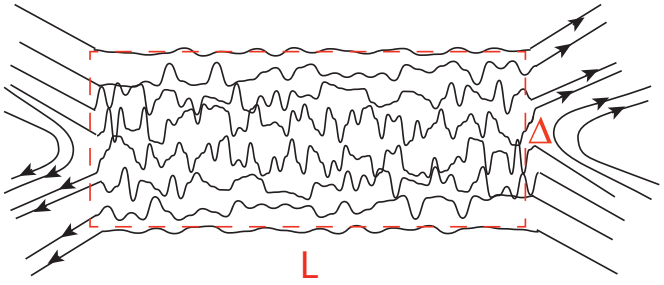

Figure 3. Sketch of turbulent reconnection configuration in the XY-plane. This could be thought of as a turbulent analog of the Sweet–Parker model. The red box shows the turbulent dissipation regime with length L and width Δ.
(A color version of this figure is available in the online journal.)

stating that hyper-diffusion is the lowest order contribution of magnetic helicity density flux conserving global magnetic helicity and, at the same time, dissipating magnetic energy. We will explore this relation further in this paper.

Since the structure of turbulent helicity density flux depends on properties of the turbulence field, different turbulence fields may produce different reconnection phenomena. In this work, we present two turbulent reconnection models: noisy reconnection and Alfvén turbulent reconnection. Both models are studied in the context of reduced magnetohydrodynamics (RMHD; Strauss 1976). We assume that the horizontal component of the magnetic field changes its sign across the current sheet (Figure 2). The other component (e.g., the guide field) is assumed to be very strong in comparison to the horizontal component. The system is assumed to be translationally symmetric in the direction orthogonal to the horizontal plane. The strong guide field avoids the null point problem and justifies the assumption of incompressibility of the flow in the horizontal plane. This reconnection geometry is ideal for the application of the so-called RMHD. Our model can be thought of as a turbulent version of the SP model, so the upstream and downstream patterns look roughly like those of the SP (Figure 3).

In the noisy reconnection model, we concentrate on a turbulent system driven by external noise and make the assumption that the current sheet is nearly marginally stable to plasmoid instability (tearing-like instability) in the noisy environment. With this assumption, we make a calculation of the helicity density flux based on the joint-reflection symmetry principle (Hwa & Kardar 1992; Diamond & Hahm 1995). We show to the lowest order that there exists a Burgers-like form for the dynamical equation for helicity density, so it is possible, and indeed likely, that transport or reconnection at the marginal state is bursty. A standard closure calculation shows that the helicity density flux has a hyper-diffusive structure. The scaling of the noisy reconnection rate is also derived, which shows that the reconnection rate weakly depends on the amplitude of noise and can be fast.

In the Alfvén turbulent reconnection model, the background turbulence is assumed to be Alfvén waves. Based on a mean field closure model, the turbulent helicity density flux driven by Alfvén waves is calculated. The hyper-diffusion is shown to be an inevitable result of Alfvén wave turbulence in a system with a current gradient. By expressing the turbulent reconnection rate in terms of the power injection rate ϵ, we find that its dependence on ϵ is very weak with $V_{\rm in} \sim \epsilon^{1/12}$, quite different from the result of $V_{\rm in} \sim \epsilon^{1/2}$ in the LV99 model (Lazarian & Vishniac 1999). We will also reexamine a controversial problem in Alfvén turbulent reconnection (Kim & Diamond 2001). In Kim & Diamond (2001), it was argued that the dissipation of the reconnecting magnetic field was strongly constrained by the conservation of the mean-square magnetic potential. Consequently, the reconnection rate remained comparable to the SP result. By including the triplet coupling term in the evolution equation for the mean-square magnetic potential, we show that when the magnetic Reynolds number is larger than a critical value, the reconnection rate could be effectively independent of Spitzer resistivity. Because of the fast turbulent dissipation of mean magnetic field energy, it can reach a much higher value than the SP model. Here, we should mention that the critical magnetic Reynolds number depends on the structure of both the reconnecting and the fluctuating fields.

Another interesting property of these two approaches is the critical behavior. For noise-induced reconnection, it is the critical current gradient scale length. For the Alfvén wave turbulent reconnection, it is the critical magnetic Reynolds number $R_{m,c}$, with $R_m = \tilde{V}_A l/\eta$ ($\tilde{V}_A$ is the Alfvén velocity set by fluctuation field $\tilde{B}$, and l is its characteristic cross-layer length scale). For fixed injection power, $R_{m,c}$ is determined by the inhomogeneity of the reconnecting field. Once the local magnetic Reynolds number exceeds $R_{m,c}$, fast reconnection occurs. Then the inhomogeneity of the reconnecting field decreases as $R_{m,c}$ increases. For $R_m < R_{m,c}$, collisional resistivity plays a dominant role in mean magnetic field energy dissipation, and the system enters a slow reconnection regime. On the other hand, the inhomogeneity of the reconnecting field can also increase due to dynamic evolution of large-scale fields, to consequently reduce $R_{m,c}$ to the point where the fast reconnection condition $R_m > R_{m,c}$ is satisfied. This property is plausible for explaining bursty phenomena, such as solar flares. It should be emphasized here that $R_{m,c}$ is only a statistical quantity. It depends on the ensemble-averaged characteristic of the turbulent magnetic field, so the critical condition for fast reconnection need not be satisfied everywhere at the same time.

The remainder of this paper is organized as follows. In Section 2, the relation between magnetic helicity density dynamics and reconnection is presented in the context of the RMHD model. The hyper-diffusive form of the helicity density flux is also discussed. In Section 3, the noise-induced reconnection approach is discussed. Under the drive of external noise, a hyper-diffusive form of helicity density flux is derived. The scaling of reconnection rate with the amplitude of the noise is presented. In Section 3.2, turbulent Alfvén reconnection is discussed. Assuming equipartition of turbulent kinetic and magnetic energies, magnetic hyper-diffusivity is derived. The scaling of the reconnection rate in terms of power injection rate is obtained. The criterion for fast reconnection is also determined, and a critical

magnetic Reynolds number is found. The paper concludes in Section 4 with a summary and prospects.

2. MAGNETIC RECONNECTION FROM THE VIEW OF HELICITY TRANSPORT

In this section, we will discuss the evolution of magnetic helicity density in an RMHD model (Strauss 1976). The RMHD equations are

$$\frac{\partial}{\partial t}\nabla_\perp^2\phi + \nabla_\perp\phi\times\hat{\mathbf{z}}\cdot\nabla_\perp\nabla_\perp^2\phi = \nabla_\perp A\times\hat{\mathbf{z}}\cdot\nabla_\perp\nabla_\perp^2 A + B_0\partial_z\nabla_\perp^2 A + \nu\nabla_\perp^2\nabla_\perp^2\phi + F^\phi \quad (1)$$

$$\frac{\partial}{\partial t}A + \nabla_\perp\phi\times\hat{\mathbf{z}}\cdot\nabla_\perp A = B_0\partial_z\phi + \eta\nabla_\perp^2 A. \quad (2)$$

Equation (1) is the equation of the fluid motion, relating the vorticity in $\hat{z}$ direction to Reynolds and Maxwell stresses. Equation (2) is Ohm's law, relating inductive electric fields to the current dissipation. A is the z-component of magnetic potential and represents the magnetic flux function. ϕ is the velocity stream function. The velocity and magnetic fields are related to the flux and stream function by $\tilde{\mathbf{v}} = \nabla_\perp\phi\times\hat{\mathbf{z}}$ and $\mathbf{B} = \nabla_\perp A\times\hat{\mathbf{z}}$, respectively. $\mathbf{B_0} = B_0\hat{\mathbf{z}}$ is the guide field setting in the z-direction. The magnetic field is measured in Alfvén velocity units. F^ϕ represents the effect of external driving to the vorticity evolution. With the scale separation, all quantities can be divided into two pieces: a mean field and a fluctuation. Thus, $A = \langle A\rangle + \tilde{A}$, $\phi = \tilde{\phi}$ and $\mathbf{B} = B_0\hat{z} + \langle B\rangle\hat{y} + \tilde{\mathbf{B}}$. Here $\langle B\rangle$ is the perpendicular reconnecting magnetic field and we take $|\tilde{B}| \ll |\langle B\rangle| \ll |B_0|$. The magnetic helicity density is $\mathcal{H} = \langle\mathcal{H}\rangle + \tilde{\mathcal{H}} = \langle A\rangle B_0 + \tilde{A}B_0$. It should be pointed out that Equations (1) and (2) are invariant under the gauge transformation: $A\to A + A'(t)$, $\phi\to\phi+\phi'(z,t)$ with A', ϕ' satisfying $\partial_t A' + \partial_z(-B_0\phi') = 0$. This describes the gauge symmetry of RMHD equations (Biskamp 1993). Because of the gauge freedom, a group solution (V, B) of the MHD equations corresponds to infinite groups of stream functions (ϕ, A). This property makes the definition of magnetic potential ambiguous. Since the physics result is independent of the choice of gauge, to study helicity density dynamics, a workable strategy is to fix the gauge.

The situation envisaged here is that the large-scale mean magnetic fields $\langle B\rangle$ are embedded in a turbulent background, and its direction is reversed across a current sheet (Figure 2). There is no magnetic null in this configuration, due to the existence of the guide field B_0. It is a reconnection configuration that is symmetric in the third direction ($\hat{z}$) (Greene 1988). The turbulence is excited by external noise forcing/stirring. The evolution equation for the total mean helicity density is

$$\frac{\partial}{\partial t}\int\langle\mathcal{H}\rangle d^3x + \int\nabla\cdot\left(\Gamma_H + \Gamma_H^\eta\right)d^3 = 0. \quad (3)$$

By Gauss's theorem, we have

$$\partial_t\int\langle\mathcal{H}\rangle d^3x + \oint_{S_{\rm sur}}\left(\Gamma_H + \Gamma_H^\eta\right)\cdot ds = 0, \quad (4)$$

where $\Gamma_H^\eta = -\eta\partial_x\langle\mathcal{H}\rangle$. $S_{\rm sur}$ is the surface surrounding the current sheet regime.

In the steady state

$$\left(\Gamma_H + \Gamma_H^\eta\right)_{\rm inflow}L + \left(\Gamma_H + \Gamma_H^\eta\right)_{\rm outflow}\Delta = 0. \quad (5)$$

Here $(\Gamma_H + \Gamma_H^\eta)_{\rm inflow}$ and $(\Gamma_H + \Gamma_H^\eta)_{\rm outflow}$ describe the helicity density flow at the upstream and downstream surfaces. In reconnection, helicity carried by inflowing magnetic field lines is converted to helicity carried by the outflowing magnetic field lines (see Figure 4). Their conversion rate is the divergence of helicity density flux in the diffusion regime $\nabla\cdot(\Gamma_H+\Gamma_H^\eta)_{\rm diffusion}$. Thus, we have

$$\left(\Gamma_H + \Gamma_H^\eta\right)_{\rm inflow}L = \nabla\cdot\left(\Gamma_H + \Gamma_H^\eta\right)_{\rm diffusion}\Delta L \quad (6)$$

$$\left(\Gamma_H + \Gamma_H^\eta\right)_{\rm outflow}\Delta = -\nabla\cdot\left(\Gamma_H + \Gamma_H^\eta\right)_{\rm diffusion}\Delta L. \quad (7)$$

Since Γ_H^η is negligible at the upstream and downstream surfaces, we have $\Gamma_{H,{\rm inflow}}L \simeq -V_{\rm in}\langle\mathcal{H}\rangle L$ and $\Gamma_{H,{\rm outflow}}\Delta \simeq V_{\rm out}\langle\mathcal{H}\rangle\Delta$. Clearly, Equation (5) is equivalent to the continuity condition $V_{\rm in}L = V_{\rm out}\Delta$. Since the current sheet is inhomogeneous in the x-direction, we have

$$\nabla\cdot\left(\Gamma_H + \Gamma_H^\eta\right)_{\rm diffusion} = \partial_x\left(\langle\tilde{v}_x\tilde{\mathcal{H}}\rangle + \Gamma_H^\eta\right) \simeq \frac{\langle\tilde{v}_x\tilde{\mathcal{H}}\rangle + \Gamma_H^\eta}{\Delta}, \quad (8)$$

where $\Gamma_{H,{\rm diffusion}} = \langle\tilde{\mathbf{v}}\tilde{\mathcal{H}}\rangle$. We write Γ_H instead of $\Gamma_{H,{\rm diffusion}}$ for simplicity in the following discussion. With Equations (5) and (6) (or (7)), $V_{\rm in}$ is obtained as

$$V_{\rm in} \simeq -\frac{\Gamma_H + \Gamma_H^\eta}{\langle\mathcal{H}\rangle} \simeq V_{\rm out}\frac{\Delta}{L}. \quad (9)$$

Here $\Gamma_H < 0, \Gamma_H^\eta < 0$, and $V_{\rm in} > 0$. This simple relation is the helicity conservation condition in magnetic reconnection, showing that the helicity density flux carried by the inflowing mean fields is converted to that carried by the outflowing mean fields in the course of reconnection and constituting a relaxation process for the mean field. When the turbulence is turned off, $\Gamma_H = 0$, we have

$$V_{\rm in} \simeq -\frac{\Gamma_H^\eta}{\langle\mathcal{H}\rangle} \simeq V_{\rm out}\frac{\Delta}{L}, \quad (10)$$

i.e., $V_{\rm in}$ can be derived as $V_{\rm in}\simeq V_A/\sqrt{S}$ (relation $V_{\rm out}\simeq V_A$ is used), which is just the SP reconnection rate.

For mean magnetic field energy, the evolution can be written as

$$\frac{\partial}{\partial t}\int\frac{1}{2}\langle B\rangle^2 d^3x - \int\frac{\Gamma_H}{B_0}\partial_x\langle j\rangle d^3x = -\int\eta\langle j\rangle^2 d^3x + S_B. \quad (11)$$

Here S_B is the magnetic energy injection rate. An interesting observation (Boozer 1986; Bhattacharjee & Hameiri 1986; Strauss 1986; Diamond & Malkov 2003) is that if we write Γ_H in the form $\Gamma_H = -D\partial_x\langle j\rangle$, the second term on the left-hand side (lhs) of Equation (11) makes a positive-definite contribution to the dissipation of the mean magnetic field energy. Thus, $\Gamma_H = -D\partial_x\langle j\rangle$ is the simplest form of helicity density flux with the property of conserving magnetic helicity and, at the same time, dissipating magnetic energy. This form is also consistent with Taylor relaxation, which is a current profile flattening process. In other words, the current density gradient is a source of free energy that drives the relaxation of magnetic fields by driving a

helicity density flux through, e.g., the hyper-diffusion. In turn, this helicity density flux induces a corresponding reconnection process that relaxes the free energy stored in the reconnecting field. The hyper-diffusion is the contribution to the magnetic helicity density flux with the lowest derivatives. There can also be other higher order contributors, such as $\alpha\partial_x^3\langle j\rangle$, $\beta\partial_x^5\langle j\rangle\ldots$. All these terms can conserve magnetic helicity and, at the same time, dissipate the magnetic energy. Since during magnetic relaxation we are mainly interested in the evolution of large-scale magnetic fields, hyper-diffusion is the leading contributor. The steady state can then be reached through the balance of the energy injection from the boundary and hyper-diffusion-induced dissipation in the reconnection volume.

It is worthwhile to add further discussions on Taylor relaxation. The final state of Taylor relaxation is force free, which is widely used in theory pertinent to solar and astrophysics (Parker 1979). Following the theoretical study of temporal evolution of force-free fields by Syrovatskii (1978), we can argue that the force-free state is a marginal state. Syrovatskii (1978) shows that, in the force-free state, a small perturbation may produce drastic deformation of the force-free fields. This singular behavior can destroy the force-free state and produce pinch current sheets. Within the current sheets, magnetic reconnection can occur and again relax the system back to a force-free state. This process can be repeated. This is also a reflection of global dynamics in the force-free environment. Furthermore, this oscillation near marginality is also one of our motivations to study the RMHD model, which describes the dynamics of a state that slightly deviates from the force-free state.

3. STRUCTURE OF TURBULENT HELICITY DENSITY FLUX AND FAST RECONNECTION

In this section, we discuss the structure of the turbulent helicity density flux Γ_H and the resulting scaling for the magnetic reconnection rate, in the context of two specific models. One is a helicity flux structure model (Hwa & Kardar 1992; Diamond & Hahm 1995; Diamond & Malkov 2003), and the other is an Alfvén wave turbulent transport model. Both approaches are implemented in the context of resistive RMHD. For two-dimensional (2D) resistive MHD, similar results can be obtained if we use magnetic flux conservation as the counterpart of magnetic helicity conservation in RMHD.

The helicity flux structure model is a noise-driven reconnection model for a system at the marginal state. It shares several similarities with the intensively studied plasmoid reconnection model (Biskamp 1986; Loureiro et al. 2007; Huang & Bhattacharjee 2010): (1) both are time dependent, (2) both require a critical state of the current sheet, (3) both tend toward a Lundquist-number-independent regime, and (4) both can reach a fast reconnection rate. There are also some differences. Here, the helicity flux structure model is constructed in the fluid regime, while plasmoid formation is observed in both fluid and kinetic regimes. Considering those similarities, it is interesting to study the reconnection problem by a model near the marginal state.

The Alfvén wave turbulent transport model is a fairly standard mean field model. The pre-existing turbulence is composed of Alfvén waves (Iroshnikov 1964; Kraichnan 1965; Goldreich & Sridhar 1995). In contrast to the helicity flux structure model, no marginal state is assumed in the Alfvén wave turbulent transport model. This scenario is somewhat similar to that of the LV99 model (Lazarian & Vishniac 1999) though the dynamics of that model have never been related to a mean field transport coefficient (i.e., turbulent resistivity, etc.). Since turbulent reconnection only makes sense in a weakly turbulent environment ($\langle\tilde{B}^2\rangle \ll \langle B\rangle^2$), one can use closure models to calculate the turbulent helicity density flux. Here, we adopt the compact method τ-formalism, used in Gruzinov & Diamond (1994). In Alfvén wave turbulent reconnection, we will emphasize the importance of the inhomogeneity of the reconnecting magnetic field in reaching a fast reconnection rate.

3.1. Noisy Reconnection

In this model, the current sheet is assumed to be marginally stable to plasmoid instability. Here, the plasmoid instability refers to an extension of tearing instability (Bhattacharjee et al. 2009). A numerical simulation has pointed out the role of noise in resistive MHD reconnection (Ng & Ragunathan 2011). When noise is added, plasmoids appear and fast reconnection occurs at high Lundquist numbers. But when noise is turned off, the magnetic field lines reconnect at the SP rate. This hints that noise is a possible trigger for plasmoid generation. The marginal state can exhibit certain critical behaviors and be described by a set of control parameters. Once a local gradient exceeds its critical value, the system will exhibit self-organized behavior, such as rapid and bursty transport. Particle-in-cell simulations (Che et al. 2011) observed that when the current layer gradient becomes intense enough, filamentation occurred, and the reconnection rate increased abruptly. A growing body of work is devoted to plasmoid (magnetic island) reconnection models. Resistive MHD simulations (Huang & Bhattacharjee 2010; Uzdensky et al. 2010) find that when the Lundquist number S is larger than a critical value S_c, the current sheet becomes highly unstable and small-scale plasmoids appeared. The reconnection becomes impulsive and the reconnection rate increases explosively. A linear instability analysis like that for tearing modes showed that the current sheet cannot be stable when its aspect ratio (Δ/L) exceeds a critical value. Numerical simulations (Biskamp 1986; Loureiro et al. 2007) suggested $(\Delta_c/L) \sim (1/100)$, corresponding to a critical Lundquist number $S_c \sim 10^4$. When $S > S_c$, the maximum linear growth rate of current sheet instability scales as $S^{1/4}(V_A/L)$. Since S is usually large, this growth rate is much faster than the transit rate of an Alfvén wave. The number of plasmoids scales as $S^{3/8}$ (Loureiro et al. 2007). Because of the fast growth rate, we expect that the linear period will be brief and thus the nonlinear dynamics determines the plasmoid reconnection rate. Another interesting property of the plasmoid instability is that the maximum growth rate occurs for a large wavenumber mode, which suggests that the steeper the sheet is, the more unstable it will be. Recent nonlinear simulations (Huang & Bhattacharjee 2010) showed that when $S > S_c$, the plasmoid reconnection rate exhibits a weak dependence on the level of the noise. They also observed a tendency toward the Lundquist-number-independence regime of reconnection rate.

The process described above resembles a self-organized criticality (SOC) phenomenon (Hwa & Kardar 1992), which can be thought of as an attractor state of a stochastic system. Here, the gradient scale length Δ of the current density can be viewed as a characteristic parameter characterizing the marginal state of the current sheet. As $\Delta \to \Delta_c$, the system enters a critical state with no intrinsic length or timescales, where Δ_c is the critical value of Δ. Said another way, dynamical behavior is similar at all scales. With the marginality assumption, any small deviation can enable the current gradient to exceed its critical value and trigger avalanches of current on all scales that tend to drive the local current profile to a flat one. With external drive,

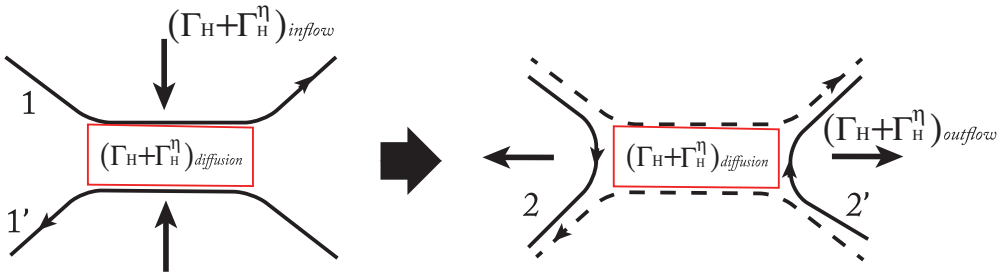

Figure 4. Illustration on the helicity flux in the XY-plane: helicity carried by reconnecting field lines 1 and 1′ is converted to the helicity carried by reconnected field lines 2 and 2′. The red box is the helicity conversion (diffusion) domain with length L and width Δ.

(A color version of this figure is available in the online journal.)

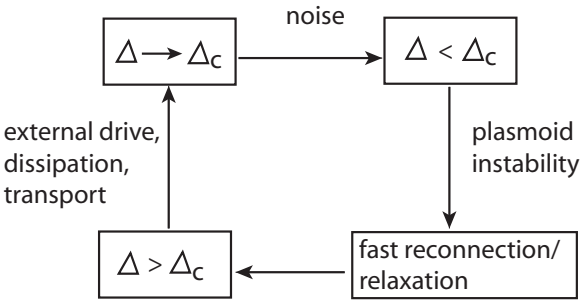

Figure 5. Marginal stability of current sheet.

dissipation, and transport, the relaxed current sheet can steepen and return to the marginal state $\Delta = \Delta_c$ again (Figure 5). In a persistently stirred system, the helicity density flux is non-steady and impulsive, reflecting the competition between these two trends. In this sense, plasmoid reconnection can be modeled as a noise-driven relaxation process near a marginal state.

When adding a small perturbation to the current sheet in the marginal state, the local current gradient will exceed the critical value. And the resulting turbulent helicity density flux may be written as a function of current density excursion $\Gamma_H = \Gamma_H(\delta j)$ (Diamond & Malkov 2003), i.e., $\delta j = j - j_c$, where j_c is the current density at the marginal state. The evolution equation for magnetic helicity density is

$$\frac{\partial}{\partial t}\delta H + \partial_x \Gamma_H(\delta j) = \eta \partial_x^2 \delta H + S_H. \tag{12}$$

Here δH is the excursion of the magnetic helicity density from the marginal state and S_H is the external noise driving the system away from the marginal state, $\langle S_H \rangle = 0$. Since both a current "void" ($\delta j < 0$) and a current "bump" ($\delta j > 0$) can produce a current gradient that exceeds the critical value, we can use the symmetry argument by Hwa & Kardar (1992): $\Gamma_H(\delta j)$ is invariant under joint-reflection symmetry: $\delta j \rightarrow -\delta j$ and $x \rightarrow -x$. As shown in Figure 6, it means that absorbing a current "void" is equivalent to expulsion of a current "bump." A general form of $\Gamma_H(\delta j)$ with this symmetry is

$$\Gamma_H(\delta j) = \sum_i \lambda_{2i} (\delta j)^{2i} + \sum_j \lambda_{2j+1} (\partial_x \delta j)^{2j+1} + \cdots. \tag{13}$$

Here, i, j are integers and λ_{2i}, λ_{2j+1} are dimensional parameters. Since we are mainly interested in the nonlinear process, to the lowest order, Γ_H can be approximately written as

$$\Gamma_H(\delta j) = \lambda \delta j^2. \tag{14}$$

This quadratic term is the "smoothest" of all possible nonlinear forms of Γ_H. λ is a dimensional parameter with a dimension

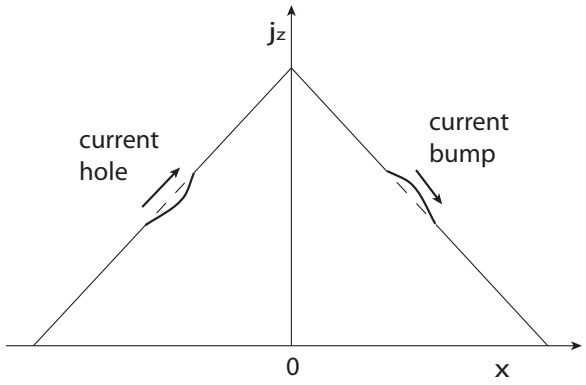

Figure 6. Joint-reflection symmetry: absorbing a current "void" is equivalent to expulsion of a current "bump."

of (velocity)(length)^3. Since the current sheet is anisotropic, $|\partial_y^2 \delta A| \ll |\partial_x^2 \delta A|$ and $\delta j \simeq -\partial_x^2 \delta A$, the evolution equation for perturbed magnetic helicity density then becomes

$$\frac{\partial}{\partial_t}\delta H + \partial_x \left[\frac{\lambda}{2}\left(\partial_x^2 \delta A\right)^2\right]^2 = \eta \partial_x^2 \delta H + S_H. \tag{15}$$

Noting that $\delta H = B_0 \delta A$, Equation (15) can be viewed as a nonlinear Ohm's law. The nonlinear term is related to the hyper-diffusive flux with a nonlinear hyper-diffusivity $D_T \simeq \lambda \delta j / B_0$, which is linearly proportional to the current excursion δj. Thus, an increase of the excursion δj will lead to an increase of both the local current gradient $\partial_x \delta j$ and the hyper-diffusivity D_T. As a result, the helicity density flux will increase faster than in a purely linear scenario. Since D_T is the coarse-grained hyper-diffusivity, it is also independent of the Spitzer resistivity η. The structural similarity between Equation (15) and the Burgers equation suggests that helicity density transport near the marginal state is intermittent and episodic. Some detailed analysis shows that there are indeed soliton-like solutions to Equation (15) (Diamond & Malkov 2003). The appearance of coherent structures bears some similarities to current sheet fragmentation or plasmoid formation.

Here, we study Equation (15) by applying the standard direct-interaction approximation (DIA) closure scheme. The purpose is to analyze the structure of the nonlinear helicity density flux and derive a scaling for the reconnection rate. Fourier transforming Equation (15) yields

$$-i\omega_k H_{\substack{k \\ \omega}} + ik\frac{\lambda}{2}\sum_{k',\omega'} k'^2 H_{\substack{-k' \\ -\omega'}} (k+k')^2 H_{\substack{k+k' \\ \omega+\omega'}} + (\eta k^2) H_{\substack{k \\ \omega}} = S_{H\,\substack{k' \\ \omega'}}. \tag{16}$$

For simplicity, we write δH as H. Substituting $H_{\substack{k+k'\\ \omega+\omega'}}$ as $H^{(2)}_{\substack{k+k'\\ \omega+\omega'}}$, one can close Equation (16) with

$$H^{(2)}_{\substack{k+k'\\ \omega+\omega'}} = L_{\substack{k+k'\\ \omega+\omega'}}\left(-\frac{i\lambda}{2}(k+k')k'^2 H_{k'}k^2 H_k\right) \tag{17}$$

$$L^{-1}_{\substack{k+k'\\ \omega+\omega'}} = -i(\omega+\omega') + \eta(k+k')^2 + d_{\substack{k+k'\\ \omega+\omega'}}. \tag{18}$$

$L_{\substack{k+k'\\ \omega+\omega'}}$ is the renormalized response function, and $d_{\substack{k+k'\\ \omega+\omega'}}$ refers to the propagator renormalization. Equation (16) is then

$$-i\omega H_{\substack{k\\ \omega}} + k\frac{\lambda}{4}\sum_{k',\omega'}(k+k')^3|H_{\substack{k'\\ \omega'}}|^2 L_{\substack{k+k'\\ \omega+\omega'}}k^2 H_{\substack{k\\ \omega}} + (\eta k^2)H_{\substack{k\\ \omega}} = S_{H\substack{k\\ \omega}}. \tag{19}$$

Taking the hydrodynamic limit $k, \omega \to 0$ and noting that parity forces cancellation of the k' contribution then yields

$$-i\omega H_{\substack{k\\ \omega}} + k^4 D_T H_{\substack{k\\ \omega}} + \eta k^2 H_{\substack{k,\\ \omega}} = S_{H\substack{k\\ \omega}} \tag{20}$$

$$D_T \simeq \frac{3\lambda^2}{4} Re\left[\sum_{k',\omega'} k'^4 |H_{\substack{k'\\ \omega'}}|^2 L_{k',\omega'}\right]. \tag{21}$$

Here, D_T is the turbulent hyper-diffusion coefficient, a function of the strength of the fluctuations. Making use of $H_{k',\omega'} = L_{\substack{k'\\ \omega'}} S_{H\substack{k'\\ \omega'}}$, one can write D_T as a function of the noise level

$$D_T \simeq \frac{3}{4}\lambda^2 \sum_{k',\omega'} \frac{k'^6 |S_{H\substack{k'\\ \omega'}}|^2 k'^4 D_T}{[\omega'^2 + (k'^4 D_T)^2]^2}. \tag{22}$$

Since we are interested in the large magnetic Reynolds number regime ($R_m \gg 1$), the resistivity is neglected. White noise $|S_{H\substack{k'\\ \omega'}}|^2 = S_0^2$ is assumed with the dimension of (velocity)(length)^2. By $\int_{-\infty}^{+\infty} dx/(1+x^2)^2 = \pi/2$, the ω'-integral can be performed to get

$$D_T \simeq \frac{3\pi\lambda^2 S_0^2}{8D_T^2}\int_{k_{\min}}^{\infty}\frac{dk'}{k'^2}. \tag{23}$$

The integral over k' is divergent as $k' \to 0$ and therefore should be cut off at a scale corresponding to $k_{\min}$, longer than the observed system scale k^{-1}, i.e., $k_{\min}^{-1} < k^{-1}$. For reconnection, the observed scale is in the same order with the width of the macroscopic current sheet. Otherwise, the coarse graining is inappropriate. For the coarse-graining procedure

$$D_T \simeq \left(\frac{3\pi\lambda^2 S_0^2}{8}\right)^{1/3} k_{\min}^{-1/3}, \tag{24}$$

where D_T is infrared divergent. Diamond & Hahm (1995) obtained a scaling for the turbulent diffusivity $D \sim k_{\min}^{-1}$, stronger than Equation (24). The reason is that the nonlinear term of Equation (3) of Diamond & Hahm (1995) does not include derivatives of the excursion field, while in Equation (13) the nonlinear term is the quadratic in the *second* derivative of the excursion field. Thus, small scales are more important in Equation (15) than in Diamond & Hahm (1995). Since infrared divergence originates mainly from large-scale dynamics, we understand why the infrared divergence of Equation (15) is weaker than the one derived in Diamond & Hahm (1995). However, the scaling of Equation (24) still indicates the possibility of anomalous transport scaling, since infrared divergence persists. This scale dependence of D_T implies a transport scaling: $\langle \delta x^2\rangle^{1/2} \sim t^{3/11}$, slower than the diffusive scaling $\langle \delta x^2\rangle^{1/2} \sim t^{1/2}$. An interesting observation is that this scaling is much softer than "ballistic," $\langle \delta x^2\rangle^{1/2} \sim t$. Thus, we see that infrared divergence does not imply ballistic scaling.

We can use the helicity and mass conservation conditions,

$$V_{\rm in} H \simeq -\Gamma_{\mathcal{H}} \tag{25}$$

$$V_{\rm in} L \simeq V_A \Delta, \tag{26}$$

to derive the reconnection rate, where the resistive part Γ_H^{η} is neglected. It can be shown that Equation (25) is equivalent to Equation (11). Writing $S_B \sim V_{\rm in}\langle B\rangle^2 L$, $-\int(\Gamma_H/B_0)\partial_x\langle j\rangle d^3x \sim (\Gamma_H/B_0)(\langle B\rangle/\Delta^2)\Delta L$ and neglecting the resistive dissipation term, we have $(\Gamma_H/B_0)(\langle B\rangle/\Delta^2)\Delta L \sim V_{\rm in}\langle B\rangle^2 L$, the same as Equation (25). From previous discussions, $\Gamma_H(\delta j) \simeq k^3 D_T \mathcal{H}/B_0 \simeq (D_T/\Delta^3)\mathcal{H}/B_0$, $V_{\rm in}$ can be derived as

$$V_{\rm in} \simeq V_A\left(\frac{D_T}{V_A L^3}\right)^{1/4}. \tag{27}$$

Using the expression for D_T, one gets

$$V_{\rm in} \sim V_A\left(\frac{\lambda^2 S_0^2}{V_A^3 L^8}\right)^{1/11}. \tag{28}$$

For reconnection, the observed scale is in the same order with the width of the macroscopic current sheet, $k^{-1} \simeq \Delta$. Then, we have $k_{\min}^{-1} < \Delta$. Nevertheless, for the purpose of the scaling discussion, we can simply set $k_{\min}^{-1} \simeq \Delta$ in Equation (24). It is the scaling of $V_{\rm in}$ for noisy reconnection near the marginal state. The most interesting property of the noisy reconnection rate is its very weak dependence on the amplitude of the white noise S_0^2, indicating that the role of the noise in noisy reconnection is quite different from that of turbulent dissipation. In noisy reconnection, it may be understood as the trigger for, or facilitator of, reconnection. Once the field lines reconnect, the subsequent relaxation process by helicity transport is driven by large-scale current gradient fields, not the noise. In this sense, the reconnection rate is insensitive to the amplitude of the noise. This is in contrast to turbulent dissipation, where the relaxation process is facilitated by turbulent scrambling, and the magnetic energy dissipation rate is linearly proportional to the rate of power injection.

Compared with the plasmoid reconnection model, noisy reconnection bears some similarities. Both exhibit critical behavior: in plasmoid instability reconnection, there exists a critical Lundquist number; in noisy reconnection, we also assume that there is a critical current density gradient length that demands the marginality of the current sheet. Differences are that, however, in noise reconnection, plasmoid turbulence is triggered/driven by external noise, but not internal instabilities. Its amplitude is determined by the level of noise. The plasmoid instability, on the other hand, is driven by the internal free energy (Bhattacharjee et al. 2009), and its amplitude is determined by the nonlinear saturation mechanism of the system. Here, the plasmoid picture is just an easier way to visualize/illustrate structures in noisy reconnection, and therefore our model is not equivalent to plasmoid reconnection. It can be regarded as a physical model for the effect of turbulent plasmoids on reconnection. We then

in this model show the physical role of noise in driving fast reconnection: for a marginally stable current sheet, noise can trigger multi-scale dynamics that drive a fast, "coarse-grained" diffusion of current density.

To make further progress in understanding the scaling of $V_{\rm in}$, we need to know the form of the dimensional parameter λ. In the resistive MHD model, we can make a simple dimensional estimation, $\lambda \sim V_A L^3$, where V_A, L are the Alfvén velocity and characteristic scale length of the system, respectively. We offer a caveat—this is not the only choice! For example, we can also take $\lambda \sim \eta L^2$ or, more generally, $\lambda \sim (\eta L^2)^\alpha (V_A L^3)^{1-\alpha}$. Here, we made the choice $\alpha = 0$ since λ comes from nonlinear processes and reflects the dynamics at scales larger than the resistive scale. Substituting λ into Equation (28), we obtain

$$V_{\rm in} \sim V_A \left(\frac{S_0^2}{V_A L^2}\right)^{1/11}, \tag{29}$$

where $S_0^2/V_A L^2$ is the relative amplitude of the noise. Since "magnetic reconnection" makes sense only when there is a smooth unperturbed topology of the reconnecting magnetic fields, $S_0^2/V_A L^2 < 1$. Because of the very weak dependence of $V_{\rm in}$ on it, the reconnection is fast. The possibility of fast reconnection can also be seen from the scaling of the effective width of the current sheet, $\Delta \sim L(S_0^2/V_A L^2)^{1/11}$. Because of the small size of the exponent, Δ could be approximately the same order as the current sheet length scale L. Thus, the current profile will be strongly broadened by the noise in the marginal state. This may reflect the effect of the current sheet filaments or plasmoids. Once there appear some coherent structures, these structures can scatter out and effectively enlarge the volume of magnetic energy dissipation to increase the reconnection rate. This broadening effect is observed in certain previous simulations (Drake et al. 1994; Che et al. 2011).

From Equation (11), we can also derive a scaling of the reconnection time. Substituting $\Gamma_H = -D_T \partial_x \langle j \rangle$ into Equation (11) yields

$$\frac{\partial}{\partial t}\int \frac{1}{2}\langle B\rangle^2 d^2x \simeq -D_T \int \left(\partial_x^2 \langle B\rangle\right)^2 d^2x - \eta \int (\partial_x \langle B\rangle)^2 d^2x. \tag{30}$$

The integrated volume on the lhs and the right-hand side (rhs) is approximately L^2 and ΔL, respectively. Neglecting collisional resistive dissipation, one gets

$$\frac{\langle B\rangle^2}{\tau_{\rm rec}} L^2 \sim D_T \frac{\langle B\rangle^2}{\Delta^4}\Delta L. \tag{31}$$

The reconnection time is given by

$$\tau_{\rm rec} \sim \frac{L}{V_A}\left(\frac{V_A^3 L^8}{\lambda^2 S_0^2}\right)^{1/11} \tag{32}$$

inversely with the noise level $(S_0^2)^{1/11}$ and consistent with the previous discussion of $V_{\rm in}$. Actually, substituting $\lambda \sim V_A L^3$ into $\tau_{\rm rec}$, one gets $\tau_{\rm rec} \sim \tau_A (V_A L^2/S_0^2)^{1/11}$, where $\tau_A = L/V_A$ is the Alfvén wave transit time. Clearly, $\tau_{\rm rec}$ is very much shorter than the SP reconnection time $\tau_{\rm SP} \sim (\tau_A \tau_\eta)^{1/2}$, where $\tau_\eta \sim L^2/\eta$. Thus, it can be said that noisy reconnection at the marginal state could indeed reach a high speed. Another characteristic worth mentioning is that the predicted reconnection rate is independent of the critical parameter Δ_c. The predictions given here are testable by numerical simulations.

3.2. Alfvén Wave Turbulent Reconnection

In this subsection, we discuss turbulent Alfvén wave reconnection. Here, the turbulence is weakly stirred by an external force at large scales. By weak stirring, we mean $\langle \tilde{B}^2\rangle \ll \langle B\rangle^2$. At the same time, the turbulent mixing of the reconnecting fields is much stronger than collisional resistive dissipation. In RMHD, the turbulent helicity density flux is $\Gamma_H = ik_y \langle \phi_k A_{-k}\rangle B_0$. Therefore, we need only to calculate the cross-correlation $\langle \phi_k A_{-k}\rangle$. In the reconnection configuration, the inhomogeneity of the reconnecting field has a non-negligible influence on the structure of the fluctuations. Generally, we can divide velocity and magnetic fluctuations into two pieces, $\tilde{v} = \tilde{v}^{(0)} + \tilde{v}^{(1)}$ and $\tilde{B} = \tilde{B}^{(0)} + \tilde{B}^{(1)}$. The zeroth and first orders are the homogeneous and inhomogeneous pieces, respectively. Thus, magnetic helicity density flux $\Gamma_H = \Gamma_H^{(0)} + \Gamma_H^{(1)}$ with $\Gamma_H^{(0)} = ik_y \langle \phi_k^{(0)} A_{-k}^{(0)}\rangle B_0$ and $\Gamma_H^{(1)} = ik_y \langle \phi_k^{(0)} A_{-k}^{(1)}\rangle B_0 + ik_y \langle \phi_k^{(1)} A_{-k}^{(0)}\rangle B_0$. Here, we assume that to lowest order the system is in a state of balanced Alfvén wave turbulence, i.e., $\langle \phi_k^{(0)} A_{-k}^{(0)}\rangle = 0$. Thus, we have

$$\langle \phi_k A_{-k}\rangle \simeq \frac{\delta \langle \phi_k A_{-k}\rangle}{\delta t}\tau_{\phi A} \simeq (\langle \partial_t \phi_k A_{-k}\rangle + \langle \phi_k \partial_t A_{-k}\rangle)\tau_{\phi A}. \tag{33}$$

Here $\tau_{\phi A}$ is the correlation time between ϕ and A (Pouquet et al. 1976; Diamond et al. 2010). Substituting the Fourier forms of Equations (1) and (2) into Equation (33), we obtain

$$\langle \phi_k A_{-k}\rangle = \tau_{\phi A,k}\left[\frac{-ik_y}{k^2} I_k^A \partial_x^3 \langle A\rangle + (-ik_y)\left(I_k^A - I_k^\phi\right)\partial_x \langle A\rangle + ik_z B_0 \left(I_k^A - I_k^\phi\right)\right] - (\nu+\eta)\tau_{\phi A,k} k^2 \langle \phi_k A_{-k}\rangle. \tag{34}$$

The first term on the rhs of Equation (34) is related to hyper-diffusion. The second term is related to turbulent diffusion. The third term is related to the Alfvén wave effect due to the guide field and vanishes after summation over k_z. The last term is related to collisional dissipation. Because of the equipartition tendency between turbulent magnetic and kinetic energies, the residual energy $-k^2(I_k^A - I_k^\phi)$ is very small and negligible (Kim & Diamond 2001). An explicit way to see this tendency toward equipartition is by using the Elsässer variables $z^+ = v + B$ and $z^- = v - B$. The residual energy can be written as $(1/2)(|v_k|^2 - |B_k|^2) = (1/2)\langle z_k^+ \cdot z_k^-\rangle$. The equipartition time at mode k is just the overlap time between two oppositely moving Alfvén wave packets. This "collision" time is on the order of $|B_{<k} k|^{-1}$ ($B_{<k}^2 = \sum_{|k'|<|k|} |B_{k'}|^2$), where $B_{<k}$ is the local Alfvén velocity of the mode k. Thus, smaller scale fluctuations can reach an equipartition state in a shorter "collision" time. The Alfvén effect was confirmed by Pouquet et al. (1976). Using the equipartition assumption, Equation (34) can be simplified to

$$\langle \phi_k A_{-k}\rangle \simeq \frac{\frac{ik_y}{k^2}\tau_{\phi A,k} I_k^A}{1 + (\nu+\eta)\tau_{\phi A,k} k^2}\partial_x \langle j\rangle. \tag{35}$$

The corresponding turbulent helicity density flux is

$$\Gamma_H \simeq -\sum_k \frac{\frac{k_y^2}{k^2}\tau_{\phi A,k} I_k^A}{1 + (\nu+\eta)\tau_{\phi A,k} k^2} B_0 \partial_x \langle j\rangle. \tag{36}$$

Here Γ_H is proportional to the intensity of the small-scale fluctuations. An important property of Γ_H is $\Gamma_H \sim \partial_x \langle j\rangle$,

indicating that the transport of helicity density is being driven by the gradient of current density, not the gradient of magnetic flux. This is a clue that the current diffusion (hyper-diffusion) plays an important role in turbulent magnetic reconnection. The collisional part of Γ_H involves $(\nu+\eta)k^2\tau_{\phi A,k} \simeq \tau_{\phi A}/\tau_\eta \simeq R_m^{-1}$, where $\tau_\eta \simeq (\nu+\eta)k^2$ is the collisional dissipation timescale and R_m is the magnetic Reynolds number. We are mainly interested in the large R_m regime, i.e.,

$$\Gamma_H \simeq -\sum_k \frac{k_y^2}{k^2}\tau_{\phi A,k} I_k^A B_0 \partial_x \langle j\rangle. \tag{37}$$

We can then obtain the steady reconnection rate by using the helicity density and mass conservation conditions

$$\Gamma_H + \Gamma_H^\eta = -V_{\rm in}\langle \mathcal{H}\rangle \tag{38}$$

$$V_{\rm in} L = \langle V_A\rangle \Delta. \tag{39}$$

Here $\Gamma_H \simeq D_T(\langle B\rangle/L_B^2)B_0$ and $\Gamma_H^\eta \simeq \eta\langle B\rangle B_0$. $L_B = |(\partial \ln\langle B\rangle/\partial x)|^{-1}$ is the gradient scale length of the reconnecting field. We retain the resistive part Γ_H^η for the purpose of discussing the crossover between the SP and hyper-diffusion reconnection models. Using the approximation $L_B \simeq \Delta$, we then obtain

$$V_{\rm in}^4 - \frac{\eta\langle V_A\rangle}{L}V_{\rm in}^2 - \frac{D_T\langle V_A\rangle^3}{L^3} = 0. \tag{40}$$

Then $V_{\rm in}$ can be obtained directly as

$$V_{\rm in}^2 = \frac{\frac{\eta\langle V_A\rangle}{L} + \sqrt{\left(\frac{\eta\langle V_A\rangle}{L}\right)^2 + 4\left(\frac{D_T\langle V_A\rangle^3}{L^3}\right)}}{2}. \tag{41}$$

A critical hyper-diffusivity $D_{T,c}$ can then be derived by comparing $(\eta\langle V_A\rangle/L)^2 \simeq D_{T,c}\langle V_A\rangle^3/L^3$. Thus, we have $D_{T,c} \simeq \eta^2 L/\langle V_A\rangle$. When $D_T \ll D_{T,c}$,

$$V_{\rm in} \simeq \left(\frac{\eta\langle V_A\rangle}{L}\right)^{1/2} = \langle V_A\rangle S^{-1/2}, \tag{42}$$

which is the SP reconnection rate. When $D_T \gg D_{T,c}$,

$$V_{\rm in} \simeq \langle V_A\rangle\left(\frac{D_T}{L^3\langle V_A\rangle}\right)^{1/4}, \tag{43}$$

which shows that the reconnection is set by hyper-diffusion. To make a further estimate of the form of D_T, we need to know the cross-correlation time $\tau_{\phi A}$. This can be obtained using a closure model for turbulence. Here, we adopt the result of the EDQNM closure (Pouquet et al. 1976; Diamond et al. 2010)

$$\tau_{\phi A} \simeq \frac{\tau_{\rm nl}}{\tau_{\rm nl}^2/\tau_A^2 + 1}, \tag{44}$$

where $\tau_{\rm nl}^{-1} \sim \langle\tilde{v}^2\rangle^{1/2} l$ is the eddy turnover time, l is the characteristic wavelength, and $\kappa = \tau_A/\tau_{\rm nl}$ is the Kubo number of the turbulence, related to the strength of memory in the system. Kubo number measures the relative importance of nonlinear and linear interaction. The Kubo number for magnetic perturbations may be defined as $\kappa \simeq (\delta B/B_0) l_\parallel/l_\perp$. For $\kappa \gg 1$, the nonlinear interaction dominates over linear wave effects; for $\kappa \ll 1$, the nonlinear cascade or dissipation process will be strongly constrained by the linear wave effect. For $\kappa \simeq 1$, the system will be in a critically balanced state, where these two effects are comparable (Goldreich & Sridhar 1995). Kadomtsev and Pogutse (Kadomtsev & Pogutse 1979) have predicted in 1979 that $\kappa \simeq 1$ should be the "natural state" for MHD turbulence. These predictions seem to have been at least partially vindicated by subsequent research (Goldreich & Sridhar 1995; Maron & Goldreich 2001). Using the standard expression for the Kubo number, we can rewrite $\tau_{\phi A}$ as $\tau_{\phi A} \sim \tau_{\rm nl}(\kappa^2/1+\kappa^2)$. Then $\Gamma_H = -D_T\partial_x\langle j\rangle$ and Equation (44) yields

$$D_T \simeq \frac{\kappa^2}{1+\kappa^2} l^3 \langle\tilde{B}^2\rangle^{1/2} B_0. \tag{45}$$

As a consequence, $V_{\rm in}$ becomes

$$V_{\rm in} \sim \langle V_A\rangle\left(\frac{\kappa^2}{1+\kappa^2}\right)^{1/4}\left(\frac{l}{L}\right)^{3/4}\left(\frac{\langle\tilde{B}^2\rangle}{\langle B\rangle^2}\right)^{1/8}, \tag{46}$$

where $(\langle\tilde{B}^2\rangle/\langle B\rangle^2)^{1/8}$ is the relative energy of the fluctuation fields. Its dependence on the fluctuation level is slightly stronger than that for noisy reconnection, but still weak. Since $\tau_A^{-1} \simeq k\cdot(\langle B\rangle\hat{y} + B_0\hat{z}) = k_y\langle B\rangle + k_z B_0$, the three-dimensional (3D) effect of the guide field is included in the Kubo number κ. As B_0 increases, $\tau_{\phi A}$ decreases and, consequently, the reconnection rate decreases, too. Though in most cases for Alfvén wave turbulence, $\kappa \simeq 1$(critical balance) is usually assumed, (deep in the inertial range) $\kappa \neq 1$ is still possible. We can then rewrite $V_{\rm in}$ in terms of the power injection rate, using $\langle\tilde{v}^2\rangle^{1/2} \simeq \langle\tilde{B}^2\rangle^{1/2} \sim \epsilon^{1/3} l^{1/3}$, as

$$V_{\rm in} \sim \langle V_A\rangle\left(\frac{\kappa^2}{1+\kappa^2}\right)^{1/4}\left(\frac{l}{L}\right)^{3/4}(\langle V_A\rangle)^{1/4} l^{1/12}\epsilon^{1/12}. \tag{47}$$

At this point, it is interesting to make a comparison with the result of the LV99 model. In our model, the reconnection rate scales with the injected power rate as $V_{\rm in} \sim \epsilon^{1/12}$—much weaker than the LV99 prediction of $V_{\rm in} \sim \epsilon^{1/2}$ (Kowal et al. 2009). For a weakly turbulent system ($\epsilon \ll 1$), the so-called turbulent reconnection cannot possibly be fast in the case of a large exponent. This difference may be related to the role of fluctuations in these two models. In the LV99 model, the turbulent reconnection rate is derived through studying the random wandering of the reconnecting field lines and happens to be sensitive to the injected power. In our model, the fluctuation fields act only as a "trigger" of the reconnection and accelerate the reconnection by driving a net turbulent helicity density flux across the boundary of the current sheet. Put another way, when the amplitude of the fluctuations becomes smaller, the turbulent energy flux could still be large enough to support a fast magnetic energy dissipation process.

The next question is, how is the hyper-diffusivity constrained by the conservation of the mean-square magnetic potential? It was demonstrated by Kim & Diamond (2001) that, in the steady state, the helicity density flux term is balanced by the collisional resistive dissipation term in the evolution equation for the mean-square magnetic potential. Consequently, the turbulent diffusivity or hyper-diffusivity is constrained to the same order as collisional resistivity, and so the original SP scaling persists. Thus, it was concluded that the small-scale fluctuations cannot result in a fast reconnection rate. Since the inhomogeneity of the current sheet can drive a finite-square magnetic potential flux

and then open another "channel" to balance magnetic helicity density flux, we reexamine this constraint by including the triplet coupling term in the budget equation for the mean-square magnetic potential. This is neglected in Kim & Diamond (2001), due to the assumption of periodic boundary conditions. Mean-square magnetic potential evolution is given by

$$\frac{1}{2}\frac{\partial H_A}{\partial t}+\frac{1}{2}\partial_x\Gamma_{A^2}=-\langle\tilde{v}_x\tilde{A}\rangle\frac{\partial\langle A\rangle}{\partial x}-\eta\langle\tilde{B}^2\rangle, \tag{48}$$

where $H_A=\langle\tilde{A}^2\rangle$ and $\Gamma_{A^2}=\langle\tilde{v}_x\tilde{A}^2\rangle$. In steady state, there are two channels in Equation (48) that can balance the turbulent helicity density flux term. One is the square magnetic potential flux term, and the other is the collisional dissipation term. The inhomogeneity of the reconnecting field is critical in determining which channel is dominant. It should be pointed out that the inhomogeneity (L_B) of the reconnecting field is mesoscale, i.e., $l_T<L_B<L_{\rm global}$, where L_T is the characteristic scale of turbulence and $L_{\rm global}$ is the characteristic scale of the global mean field.

First, we give a derivation of the constraint on D_T when $\partial_x\Gamma_{A^2}$ is negligible ($|\partial_x\Gamma_{A^2}|\ll|\eta B^2|$). In this limit, Equation (48) becomes

$$\frac{1}{2}\frac{\partial H_A}{\partial t}=-\langle\tilde{v}_x\tilde{A}\rangle\frac{\partial\langle A\rangle}{\partial x}-\eta\langle\tilde{B}^2\rangle. \tag{49}$$

In steady state

$$\langle\tilde{v}_x\tilde{A}\rangle\frac{\partial\langle A\rangle}{\partial x}+\eta\langle B^2\rangle=0. \tag{50}$$

Substituting $\langle\tilde{v}_x\tilde{A}\rangle=-D_T(\partial^3\langle A\rangle/\partial x^3)$ into Equation (50) yields

$$\frac{\langle\tilde{B}^2\rangle}{-\langle B\rangle\partial_x^2\langle B\rangle}=\frac{D_T}{\eta}. \tag{51}$$

This is the Zeldovich relation for the hyper-diffusivity. With $\partial_x^2\langle B\rangle\simeq(\langle B\rangle/L_B^2)$, D_T becomes

$$\frac{D_T}{\eta L_B^2}\simeq\frac{\langle\tilde{B}^2\rangle}{\langle B\rangle^2}. \tag{52}$$

This result gives the universal scaling relation of D_T in terms of collisional resistivity η, the reconnecting field length scale L_B, and the relative amplitude of the fluctuation field $\tilde{B}^2/\langle B\rangle^2$. Given the plausible assumption that L_B is independent of η, D_T is constrained to a low value when η is very small. We can also define an effective magnetic Reynolds number as the ratio of relaxation-induced helicity transport to collisional resistive dissipation of helicity, i.e.,

$$R_{m,\rm eff}\simeq\frac{D_T L_B^{-4}}{\eta L_B^{-2}}\sim\frac{\langle\tilde{B}^2\rangle}{\langle B\rangle^2}. \tag{53}$$

For weak turbulence, $R_{m,\rm eff}<1$. So, for the weakly inhomogeneous system, the dynamics will be limited to a low $R_{m,\rm eff}$ and the corresponding reconnection rate cannot reach a large value. This is also the argument made by Kim & Diamond (2001), which is valid for global dissipation (i.e., a neutral layer).

However, strong magnetic inhomogeneity is a key characteristic of the reconnecting field, and its contribution to Γ_{A^2} should be included in Equation (48). Indeed, for small L_B, the triplet coupling term could exceed the collisional dissipation term and balance the helicity density flux term. To make a quantitative estimate of Γ_{A^2}, a closure calculation is needed. Here, we adopt a general method developed for inhomogeneous turbulent systems (Yoshizawa 1984; Gurcan et al. 2006), namely, the two-scale direct-interaction approximation (TSDIA). The details of the calculation are put in the Appendix. A dimensional estimate of the TSDIA result of Γ_{A^2} is

$$\Gamma_{A^2}\sim\tau_l\frac{l^2}{L_B^2}\langle\tilde{B}^2\rangle^2, \tag{54}$$

where τ_l is the characteristic triad coupling time at the characteristic wavelength l. When $|\partial_x\Gamma_{A^2}|\gg\eta\langle\tilde{B}^2\rangle$, or equivalently

$$\tau_l\frac{l^2}{L_B^2}\langle\tilde{B}^2\rangle^2\gg\eta\langle\tilde{B}^2\rangle, \tag{55}$$

the triplet coupling term will exceed the dissipation term. In steady state, Equation (48) then becomes

$$\frac{1}{2}\partial_x\Gamma_{A^2}=-\langle\tilde{v}_x\tilde{A}\rangle\frac{\partial\langle A\rangle}{\partial x}. \tag{56}$$

The constraint on D_T is obtained as

$$D_T\simeq\frac{(\partial_x\Gamma_{A^2})}{2\langle B\rangle\partial_x^2\langle B\rangle}. \tag{57}$$

For this limit, D_T is independent of the collisional resistivity or the Lundquist number. For the sake of the scaling discussion, we approximate τ_l by $\tau_{\phi A}$, since they are comparable (Diamond et al. 2010). Then, Equation (55), for the critical R_m, becomes

$$R_m\gg\left(1+\frac{1}{\kappa^2}\right)\left(\frac{L_B}{l}\right)^2. \tag{58}$$

Here $R_m=l\langle\tilde{B}^2\rangle^{1/2}/\eta$. A critical value for R_m is given by $R_{m,c}\simeq(1+1/\kappa^2)(L_B/l)^2$. $R_{m,c}$ is determined by the structure of both the external energy injection and the reconnecting field itself. For fixed external injected power, $R_{m,c}$ is solely determined by L_B. Furthermore, L_B can be viewed as a critical parameter, when ϵ is fixed. When $R_m\gg R_{m,c}$, D_T will not be constrained by η and the reconnection rate can reach a large value. For weak turbulence, $\kappa\leqslant1$. To achieve a low threshold for the fast reconnection, we can increase the inhomogeneity (L_B^{-1}) or the injection scale of noise forcing/stirring (l). When $R_m\ll R_{m,c}$, $V_{\rm in}$ will revert to the result of Kim & Diamond (2001).

We already discussed the role of fluctuations in reconnection. One related question is how to sustain the turbulent environment—i.e., are there mechanisms other than external stirring? Put alternatively, after the lengthy discussion of the effect of turbulence on reconnection, we now turn to the question of the *impact of reconnection on turbulence*. This is important for the system to remain in a persistent state of fast reconnection. Here we suggest a heuristic answer to this question. From Equations (1) and (2), we obtain the evolution equations for turbulent kinetic energy E_K and magnetic energy E_B:

$$\begin{aligned}\frac{\partial E_K}{\partial t}&=\frac{1}{2}\frac{\partial}{\partial t}\int|\nabla_\perp\tilde{\phi}|^2d^3x\\&=\int\langle\tilde{\phi}\partial_y\nabla_\perp^2\tilde{A}\rangle\partial_x\langle A\rangle d^3x-\int\langle\tilde{\phi}\partial_y\tilde{A}\rangle\partial_x^3\langle A\rangle d^3x\\&\quad-\nu\int|\nabla_\perp\tilde{\phi}|^2d^3x-\int\langle\tilde{\phi}\tilde{F}^\phi\rangle d^3x\end{aligned} \tag{59}$$

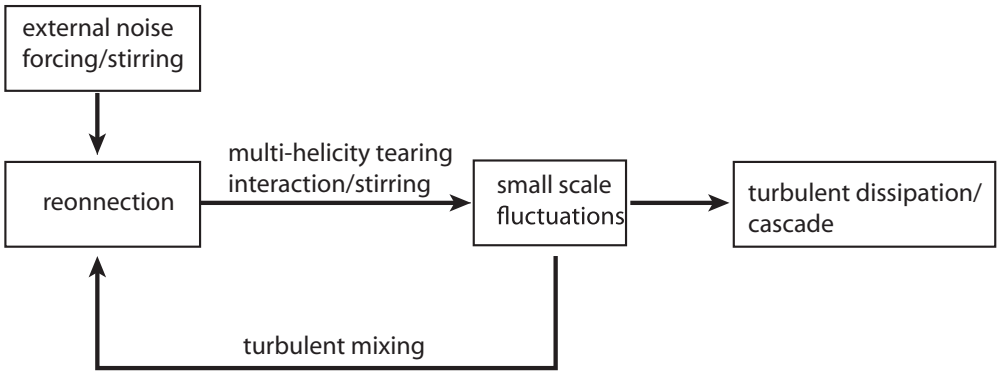

Figure 7. Energy conversion in turbulent reconnection.

$$\frac{\partial E_B}{\partial t} = \frac{1}{2}\frac{\partial}{\partial t}\int |\nabla_\perp \tilde{A}|^2 d^3x = -\int \langle \tilde{\phi}\partial_y \nabla_\perp^2 \tilde{A}\rangle \partial_x \langle A\rangle d^3x - \eta \int |\nabla_\perp^2 \tilde{A}|^2 d^3x. \quad (60)$$

Here, all the surface integrals are neglected. The first term on the rhs of Equations (59) and (60) represents energy exchange between $\tilde{v}$ and $\tilde{B}$, and they cancel each other exactly. The second term on the rhs of Equation (59) represents the force of reconnecting fields on the fluid. The last term on the rhs of Equation (59) represents external stirring. The third term of Equation (59) and the last term of Equation (60) are viscous dissipation and ohmic heating, respectively. Then, the evolution equation for total fluctuation energy is

$$\frac{\partial}{\partial t}(E_K + E_B) = -\int \langle \tilde{\phi}\partial_y \tilde{A}\rangle \partial_x^3 \langle A\rangle d^3x - \nu \int |\nabla_\perp \tilde{\phi}|^2 d^3x - \eta \times \int |\nabla_\perp^2 \tilde{A}|^2 d^3x - \int \langle \tilde{\phi}\tilde{F}^\phi\rangle d^3x. \quad (61)$$

As is shown, there are two channels to sustain a finite turbulent energy. One is by external stirring, and the other is by reconnection, which is related to $V_{\rm in}$. Without external stirring, the system may still possibly remain in a turbulent state through the balance of reconnection stirring (the first term on the rhs of Equation (61)) and classical dissipation. Substituting $\langle \tilde{\phi}\partial_y \tilde{A}\rangle = -\Gamma_H/B_0 = D_T \partial_x \langle j\rangle$ and $\partial_x^2 \langle A\rangle = -\langle j\rangle$ into the first term on the rhs of Equation (61), the production term in Equation (61) becomes

$$\frac{\partial}{\partial t}(E_K + E_B)|_{NL} = \int D_T |\partial_x \langle j\rangle|^2 d^3x > 0. \quad (62)$$

Equation (62) shows that large-scale magnetic energy dissipated in the reconnection is converted to turbulent kinetic and magnetic energy. Here the dissipation or relaxation mechanism is related to the product of the helicity flux $\langle \tilde{v}_x \tilde{A}\rangle$ (akin to the thermodynamic flux) and the current gradient (akin to the thermodynamic force). For the energy conversion mechanisms, in noisy reconnection, small-scale tearing fluctuations could be generated by multi-helicity tearing interactions of large-scale fields (Matthaeus & Lamkin 1985, 1986). In Alfvén wave turbulent reconnection, newly born Alfvén waves are produced by the "stirring" due to localized reconnection events and their coupling to reconnecting fields. In turn, the newly generated fluctuations can speed up the reconnection and relaxation process. This creates a feedback loop for turbulent reconnection (Figure 7). In this loop, the current gradient is the source of free energy. Regarding the ultimate fate of magnetic energy dissipated in the reconnection, some is coupled to small scales and dissipated through turbulent cascade or turbulent acceleration of particles (an effect not captured in the fluid model), and some may be trapped in structures such as plasmoids (which may undergo collective acceleration).

4. SUMMARY AND DISCUSSION

In this paper, we discussed the fast reconnection problem from the perspective of magnetic helicity transport in a state of preexisting turbulence, within the context of resistive RMHD. The reconnection process can be described in terms of the transport and dissipation of magnetic helicity. To quantitatively study the influence of external noise forcing/stirring on reconnection, we presented two specific models. One is a helicity flux structure model (noisy reconnection), and the other is an Alfvén wave turbulent transport model (Alfvén wave turbulent reconnection). Both are set up in weakly turbulent systems, since the turbulent reconnection problem is well posed and nontrivial only when the topology of the mean reconnecting field is unambiguous. The main results of the analysis of these two models are summarized as follows:

1. *Noisy reconnection*
   In this model, we consider a current sheet that is nearly marginally stable to plasmoid instability. Using a general symmetry principle, we analyzed all possible forms of turbulent helicity density flux and retained the lowest order approximation, $\Gamma_H(\delta j) = \lambda \delta j^2$. We performed a renormalization calculation on the nonlinear Ohm's law by a standard DIA closure scheme and found a hyper-diffusive form of Γ_H, $\Gamma_H = -D_T \partial_x \delta j$, where $D_T \simeq (3\pi\lambda^2 S_0^2/8)^{1/3} k_{\rm min}^{-1/3}$. With the assumption of $\lambda \sim V_A L^3$, we obtained the scaling of the reconnection rate $V_{\rm in} \sim V_A (S_0^2/V_A L^2)^{1/11}$. An obvious property of $V_{\rm in}$ is that it is very weakly dependent on the relative amplitude of the noise.
2. *Alfvén wave turbulent reconnection*
   In this model, we assume that the reconnecting field lines are weakly stirred by externally driven Alfvén-wave-type perturbations. Because of the tendency toward equipartition of turbulent magnetic and kinetic energy, it was demonstrated that hyper-diffusion is the dominant transport mechanism for the helicity density flux. Using a closure scheme, the τ-formalism, the scaling of the reconnection rate, $V_{\rm in} \sim \langle V_A\rangle (\kappa^2/1+\kappa^2)^{1/4} (l/L)^{3/4} (\langle V_A\rangle)^{1/4} l^{1/12} \epsilon^{1/12}$,

was derived. Again, it is weakly dependent on the external stirring, i.e., $V_{\rm in} \sim \epsilon^{1/12}$. We also discussed the constraint imposed by the conservation of the mean-square magnetic potential. In contrast to the Kim & Diamond result, we found that by including the triplet coupling term, the hyper-diffusivity can escape the limitation of the Zeldovich relation if the reconnecting field length scale L_B is small enough. This is because the strong inhomogeneity of the reconnecting field can produce a large mean-square magnetic potential flux (triplet) that can balance the helicity density flux and render the reconnection rate independent of the collisional resistivity. Using the standard TSDIA scheme, we calculated the triplet coupling term in the evolution equation for the mean-square magnetic potential and obtained a critical magnetic Reynolds number, $R_{m,c} = (1 + 1/\kappa^2)(L_B/l)^2$. When $R_m \gg R_{m,c}$, the reconnection rate is independent of the Lundquist number and is fast; when $R_m \ll R_{m,c}$, the reconnection rate is constrained by the collisional resistivity η and remains in the slow SP regime.

Through the two turbulent reconnection models, the distinction between turbulent reconnection and turbulent dissipation is demonstrated. In both processes, the magnetic energy dissipation rate can be written as ϵ^α. For turbulent reconnection, $\alpha \ll 1$, since the reconnection rate is very weakly dependent on ϵ. This property is consistent with a recent simulation (Loureiro et al. 2009) implemented for 2D resistive MHD, which observed a very weak dependence of the reconnection rate on ϵ with an exponent 0.15–0.25. For turbulent dissipation, $\alpha \sim 1$. We also gave a tentative explanation of the role of turbulence in reconnection. In turbulent reconnection, the fluctuations do not initiate the relaxation process directly but only trigger the reconnection. In contrast, in turbulent dissipation, the relaxation and the dissipation of magnetic energy are driven directly by the fluctuations. We also discussed the relation between reconnection and turbulence from the energy conversion viewpoint and argued that it is possible for the system to sustain a turbulent reconnection state self-consistently.

In view of the ubiquity of turbulence in space and astrophysical plasmas, turbulent reconnection seems likely to occur in these environments. An immediate application is the solar flare problem. As conjectured by Parker (1988), the solar corona may be heated by an ensemble of small-scale flares. Each flare is thought to represent an "intermittent" reconnection event. This conjecture is supported by observations (Lin et al. 1984). There are also phenomenological SOC-type models to explain the statistical properties of the solar flares (i.e., Lu & Hamilton 1991). The turbulent reconnection model could be a candidate for describing the dynamical process of a solar flare. In turbulent reconnection, a weak level of fluctuation can trigger a fast reconnection process, so we could expect that turbulent reconnection occurs in many sites in the solar corona. And the duration of turbulent reconnection can be at the same order with Alfvén time, and it is also short enough to explain the observations. Any theory of the solar flare should also be able to explain the slow accumulation of magnetic flux. This is an intrinsic property of our model. In noisy reconnection, it is reflected by the formation of a critical current sheet scale and, in Alfvén wave turbulent reconnection, it is reflected by the formation of a critical magnetic Reynolds number. Any of these processes could define a magnetic flux accumulation period.

In this paper, we discussed only fast reconnection in the context of resistive MHD, for quasi-2D mean field configurations. By the discussion of the physical role of the turbulence, we can expect that these approaches are still applicable to more general 3D configurations. A natural next step is to extend the current analysis to the kinetic or collisionless regimes. In fact, some tearing mode instability analysis (Baalrud et al. 2011) in the Hall-MHD regime shows that the plasmoid growth rate is larger than that for resistive MHD. We can expect that there will be similar noisy reconnection in the kinetic regime. Besides noisy reconnection, we can also derive the alternatives to Alfvén wave turbulent reconnection such as kinetic Alfvén wave or whistler wave turbulent reconnection models. The generalization to kinetic regimes is rather direct and will also broaden the applicability of these concepts. By including different kinds of kinetic turbulence at smaller scales, we may also introduce new channels to exchange electron momentum, such as wave momentum radiation and electron momentum transfer. These effects can constitute a more consistent picture of electron dynamics in reconnection. For example, the synergy of electron momentum transport (hyper-diffusivity) and electron momentum transfer (anomalous resistivity) may also act as a spatial dependence anomalous resistivity that can produce a Petschek-like reconnection rate (Kulsrud 2001). Another interesting and challenging problem is how the system approaches the marginal state (Gil & Sornette 1996). Currently, the critical current sheet is just an assumption. A nonlinear analysis is required to find the scaling of Δ_c. This problem is closely related to that of the formation mechanism of the marginal state. Another future work is to model the feedback loop of turbulence and reconnection consistently and study the conditions to reach a stable, turbulent reconnection state. We leave the study of these problems to the future.

We thank D. Ryu, J. Cho, O. D. Gurcan, L. Wang, P. C. Hsu, and the participants in the sixth Korean Astrophysics Workshop (Pohang, 2011 November) for stimulating discussions. This work was supported by the Ministry of Education, Science, and Technology of Korea via the WCI project 2009-001, the U.S. Department of Energy Grants, No. DE-FG02-04ER54738, UCSD Grant, and the CMTFO. Z. B. Guo and X. G. Wang were also supported by NSFC Grants, Nos. 40731056, 10975012, and the Graduate School of Peking University.

APPENDIX

In this Appendix, we provide some steps calculating the triplet coupling term Γ_{A^2}. More detail and physical discussion can be found in Yoshizawa (1984) and Gurcan et al. (2006).

Writing Equations (1) and (2) in Fourier forms, one has

$$\partial_t \phi_k + \left(-ik_\parallel V_A - \frac{ik_y}{k^2}\partial_x^2\langle B\rangle\right) A_k + \nu k^2 \phi_k = S_k^\phi \tag{A1}$$

$$\partial_t A_k - ik_\parallel V_A \phi_k + \eta k^2 A_k = S_k^A. \tag{A2}$$

Where S_k^{ϕ} and S_k^A are the nonlinear coupling terms,

$$S_k^{\phi} = \frac{1}{2}\sum_{\mathbf{p+q=k}} \frac{p\times\hat{z}\cdot q}{k^2}(p^2-q^2)(\phi_p\phi_q - A_pA_q)$$
$$S_k^{A} = \frac{1}{2}\sum_{\mathbf{p+q=k}} p\times\hat{z}\cdot q(A_q\phi_p - A_p\phi_q).$$

Writing them in a compact form,

$$\partial_t \eta_k^{\alpha} + H_k^{\alpha\beta}\eta_k^{\beta} = \frac{1}{2}\sum_{\mathbf{p+q=k}} M_{k,p,q}^{\alpha\beta\gamma}\eta_p^{\beta}\eta_q^{\gamma}, \tag{A3}$$

where

$$\eta_k^{\alpha} = \begin{pmatrix}\phi_k\\ A_k\end{pmatrix}, \quad H_k^{\alpha\beta} = \begin{pmatrix}\nu k^2 & -ik_{\parallel}V_A - \frac{ik_y}{k^2}\partial_x^2\langle B\rangle\\ -ik_{\parallel}V_A & \eta k^2\end{pmatrix}$$
$$M_{k,p,q}^{\alpha\beta\gamma} = \delta^{1\alpha}(\delta^{1\beta}\delta^{1\gamma} - \delta^{2\beta}\delta^{2\gamma})\frac{\mathbf{p}\times\hat{\mathbf{z}}\cdot\mathbf{q}}{k^2}(p^2-q^2) + \delta^{2\alpha}\epsilon^{\alpha\beta}\mathbf{p}\times\hat{\mathbf{z}}\cdot\mathbf{q}.$$

For small viscosity and resistivity, $(k_{\parallel}V_A/\nu k^2) \sim (\tau_{\nu}/\tau_A) \gg 1$, $(k_{\parallel}V_A/\eta k^2) \sim (\tau_{\eta}/\tau_A) \gg 1$. $H_k^{\alpha\beta}$ can be approximated as

$$H_k^{\alpha\beta} \simeq \begin{pmatrix}0 & -ik_{\parallel}V_A - \frac{ik_y}{k^2}\partial_x^2\langle B\rangle\\ -ik_{\parallel}V_A & 0\end{pmatrix}.$$

To calculate the triplet couple term Γ_{A^2}, we need to find the response function of Equation (A3).

An easier way is to rewrite Equation (A3) in a group of new variables ϕ_k^{α}. ϕ_k^{α} are related to η_k^{α} through

$$\eta_k^{\alpha} = A_k^{\alpha\beta}\Phi_k^{\beta},$$

where A_k is the transformation matrix. Substituting it into Equation (A1) yields

$$\partial_t\Phi_k^{\delta} + \left(A_k^{-1}\right)^{\delta\alpha}H_k^{\alpha\beta}A_k^{\beta\gamma}\Phi_k^{\gamma} = \left(A_k^{-1}\right)^{\delta\alpha}S_k^{\alpha}. \tag{A4}$$

Choosing proper A_k, H_k can be diagonalized as

$$\left(A_k^{-1}\right)^{\delta\alpha}H_k^{\alpha\beta}A_k^{\beta\gamma} = \lambda_k^{\delta}\delta^{\delta\gamma}, \tag{A5}$$

where λ_k^{δ} are the eigenvalues of $H_k^{\alpha\beta}$,

$$\lambda_k^1 = i\sqrt{k_{\parallel}V_A\left(k_{\parallel}V_A + \frac{k_y}{k^2}\partial_x^2\langle B\rangle\right)}, \quad \lambda_k^2 = -i\sqrt{k_{\parallel}V_A\left(k_{\parallel}V_A + \frac{k_y}{k^2}\partial_x^2\langle B\rangle\right)}.$$

The corresponding eigenvectors of $H_k^{\alpha\beta}$ are

$$\xi_k^1 = \begin{pmatrix}1\\ \frac{-ik_{\parallel}V_A}{\lambda_k^1}\end{pmatrix}, \quad \xi_k^2 = \begin{pmatrix}1\\ \frac{-ik_{\parallel}V_A}{\lambda_k^2}\end{pmatrix}.$$

With ξ_k^{α}, $A_k^{\alpha\beta}$ can be obtained as

$$A_k^{\alpha\beta} = \begin{pmatrix}1 & 1\\ \frac{-ik_{\parallel}V_A}{\lambda_k^1} & \frac{-ik_{\parallel}V_A}{\lambda_k^2}\end{pmatrix}, \quad \left(A_k^{-1}\right)^{\alpha\beta} = \frac{1}{\det A_k}\begin{pmatrix}\frac{-ik_{\parallel}V_A}{\lambda_k^2} & -1\\ \frac{ik_{\parallel}V_A}{\lambda_k^1} & 1\end{pmatrix},$$

$\det(A_k) = ik_{\parallel}V_A(1/\lambda_k^1 - 1/\lambda_k^2)$.

Then, the evolution equation of Φ_k^{α} becomes

$$\partial_t\Phi_k^{\alpha} + \lambda_k^{\alpha}\Phi_k^{\alpha} = \left(A_k^{-1}\right)^{\alpha\beta}S_k^{\beta} \tag{A6}$$

(no sum over α). This is a Langevin-type equation with a noise term $(A_k^{-1})^{\alpha\beta}S_k^{\beta}$ and can be solved directly as

$$\Phi_k^{\alpha}(t) = \int_0^t e^{-\lambda_k^{\alpha}(t-t')}\left(A_k^{-1}\right)^{\alpha\beta}S_k^{\beta}(t')dt'.$$

Using Equation (A5), the response function in ϕ_k space is obtained as

$$\eta_k^\alpha(t) = A_k^{\alpha\beta}\Phi_k^\beta(t) = \int_0^t A_k^{\alpha\beta} e^{-\lambda_k^\beta(t-t')}\left(A_k^{-1}\right)^{\beta\gamma} S_k^\gamma(t')dt' = \int_0^t R_k^{\alpha\gamma}(t,t')S_k^\gamma(t')dt', \tag{A7}$$

where $R_k^{\alpha\gamma}(t,t') = A_k^{\alpha\beta}e^{-\lambda_k^\beta(t-t')}(A_k^{-1})^{\beta\gamma}$.

We can also write $R_k^{\alpha\gamma}(t,t')$ in a compact form

$$R_k^{\alpha\gamma}(t,t') = r_k^{\alpha\beta\gamma}e^{-\lambda_k^\gamma(t-t')}, \tag{A8}$$

where

$$r_k^{\alpha\beta 1} = \frac{1}{\lambda_k^2-\lambda_k^1}\begin{pmatrix} -\lambda_k^1 & \frac{-\lambda_k^1\lambda_k^2}{ik_\parallel V_A} \\ ik_\parallel V_A & \lambda_k^2 \end{pmatrix}; \quad r_k^{\alpha\beta 2} = \frac{-1}{\lambda_k^2-\lambda_k^1}\begin{pmatrix} -\lambda_k^2 & \frac{-\lambda_k^1\lambda_k^2}{ik_\parallel V_A} \\ ik_\parallel V_A & \lambda_k^1 \end{pmatrix}.$$

By DIA, the triplet couple term is approximately

$$\Gamma_{A^2} = \langle \tilde{v}_x \tilde{A}^2\rangle \simeq -\frac{i}{3}\left\langle \sum_{\mathbf{p+q=k}} [(q_y\phi_{-q}A_{-p} + p_y\phi_{-p}A_{-q})\delta A_k - k_y A_{-p}A_{-q}\delta\phi_k]\right\rangle, \tag{A9}$$

where δA_k and $\delta\phi_k$ are produced by coherent interactions, $\delta A_k \sim \phi_p A_q, \phi_q A_p$, $\phi_k \sim \phi_p\phi_q, A_pA_q$. Their specific forms can be derived from

$$\partial_t\delta\eta_k^\alpha + H_k^{\alpha\beta}\delta\eta_k^\beta = \frac{1}{2}\sum_{\mathbf{p+q=k}}\left(M_{k,p,q}^{\alpha\beta\gamma}\eta_p^\beta\eta_q^\gamma - iP_{k,p,q}^{\alpha\beta\gamma}\partial_X\eta_p^\beta\eta_q^\gamma - iP_{k,q,p}^{\alpha\gamma\beta}\partial_X\eta_p^\beta\eta_q^\gamma\right). \tag{A10}$$

With two-scale separation $ik_x \to ik_x + \partial_X(|\partial_X| \ll |k_x|)$, we have

$$M_{k,p,q}^{\alpha\beta\gamma} \simeq M_{k,p,q}^{\alpha\beta\gamma} - iP_{k,p,q}^{\alpha\beta\gamma}\partial_X - iP_{k,q,p}^{\alpha\gamma\beta}\partial_X,$$

where $P_{k,p,q}^{\alpha\beta\gamma} = (\partial M_{k,p,q}^{\alpha\beta\gamma}/\partial p_x)$. Using the response function $R_k^{\alpha\beta}$, one obtains

$$\delta\eta_k^\alpha \simeq \frac{1}{2}\int_0^t R_k^{\alpha\lambda}(t,t')M_{k,p,q}^{\lambda\beta\gamma}\eta_p^\beta(t')\eta_q^\gamma(t')dt' - \frac{i}{2}\int_0^t R_k^{\alpha\lambda}(t,t')\left[P_{k,p,q}^{\lambda\beta\gamma}\partial_X\eta_p^\beta(t')\eta_q^\gamma(t') + P_{k,q,p}^{\lambda\gamma\beta}\partial_X\eta_p^\beta(t')\eta_q^\gamma(t')\right]. \tag{A11}$$

Substituting it into Equation (A9), after some algebra, one obtains

$$\begin{aligned}\Gamma_{A^2} = &-\frac{1}{6}\sum_{\mathbf{p+q=k}} Re\left(r_{k,p,q}^{11\mu}\theta^\mu\right)\left[\frac{-k_y}{k^2}\left(q_y(p^2-q^2) - 2p_x\mathbf{p}\times\hat{z}\cdot\mathbf{q}\right)I_q^A\partial_X I_p^A\right] \\ &-\frac{1}{6}\sum_{\mathbf{p+q=k}} Re\left(r_{k,p,q}^{22\mu}\theta^\mu\right)\left[q_y^2 I_q^\phi\partial_X I_p^A - q_y p_y I_p^A\partial_X I_q^\phi\right].\end{aligned} \tag{A12}$$

We neglected all the cross-correlation terms ($\langle\phi A\rangle \simeq 0$). θ^μ is the triad coupling time

$$\theta^\mu = \int_0^t e^{\left[-i(\omega^\mu+\omega_p+\omega_q)-(\gamma_k+\gamma_p+\gamma_q)\right](t-t')}dt' = \frac{1-e^{-i\Delta w^\mu t+\gamma_{k,p,q}t}}{-i\Delta\omega^\mu+\gamma_{k,p,q}},$$

where $\lambda_k^1 = i\omega_k^1$, $\lambda_k^2 = -i\omega_k^2$, $\Delta\omega^\mu = \omega_k^\mu + \omega_p + \omega_q$, and $\gamma_{k,p,q} = \gamma_k + \gamma_p + \gamma_q$.

For a weakly inhomogeneous system($|\partial \ln\langle B\rangle/\partial x| \ll |k|$), the disperse relations are

$$\omega_k^1 \simeq ik_\parallel V_A\left(1 + \frac{k_y\partial_x^2\langle B\rangle}{2k^2k_\parallel V_A}\right) \simeq ik_\parallel V_A, \quad \omega_k^2 \simeq -ik_\parallel V_A\left(1 + \frac{k_y\partial_x^2\langle B\rangle}{2k^2k_\parallel V_A}\right) \simeq -ik_\parallel V_A.$$

In these approximations, the resonance condition $\Delta\omega_k^1 = 0$ or $\Delta\omega_k^2 = 0$ can always be satisfied. Then, the triad couple part

$$Re\left(r_{k,p,q}^{11\mu}\theta^\mu\right) = Re\left(r_{k,p,q}^{22\mu}\theta^\mu\right) \simeq -\frac{1}{2\gamma_{k,p,q}}.$$

With equipartition condition $I_k^A \simeq I_k^\phi$, Γ_{A^2} becomes

$$\Gamma_{A^2} \simeq \frac{1}{12}\sum_{\mathbf{p+q=k}}\frac{1}{\gamma_{k,p,q}}\left[\frac{-k_y}{k^2}\left(q_y(p^2-q^2) - 2p_x\mathbf{p}\times\hat{z}\cdot\mathbf{q}\right) + q_y^2\right]I_q^A\partial_X I_p^A = \sum_p D_p^{(AA)}\partial_X I_p^A \tag{A13}$$

$$D_p^{(AA)} = \frac{1}{12}\int\int \frac{1}{\gamma_{k,p,q}}\left[\frac{-k_y}{k^2}\left(q_y(p^2-q^2) - 2p_x\mathbf{p}\times\hat{z}\cdot\mathbf{q}\right) + q_y^2\right]\delta(\mathbf{k}-\mathbf{p}-\mathbf{q})I_q^A d^3k d^3q.$$

The calculation of the integral in $D_p^{(AA)}$ is rather complex since we need to know the triad couple time and the spectrum of I_q^A, both of which depend on the specific turbulence closure models. For a scaling discussion, one can make an estimate of Γ_{A^2} as

$$\Gamma_{A^2} \sim \tau_l \frac{l^2}{L_B^2}\langle\tilde{B}^2\rangle^2, \tag{A14}$$

where l is the characteristic wavelength of Alfvén wave, τ_l is the characteristic triad couple time at l, and $L_B = |\partial \ln\langle B\rangle/\partial x| \sim |\partial \ln\langle\tilde{B}^2\rangle/\partial x|$.

REFERENCES

Armstrong, J. W., Rickett, B. J., & Spangler, S. R. 1995, ApJ, 443, 209
Baalrud, S. D., Bhattacharjee, A., Huang, Y.-M., & Germaschewski, 2011, Phys. Plasmas, 18, 092108
Bhattacharjee, A., & Hameiri, E. 1986, Phys. Rev. Lett., 57, 206
Bhattacharjee, A., Huang, Y. M., Yang, H., & Rogers, B. 2009, Phys. Plasmas, 18, 112102
Birn, J., Drake, J. F., Shay, M. A., et al. 2001, J. Geophys. Res., 106, 3715
Biskamp, D. 1986, Phys. Fluids, 29, 1520
Biskamp, D. 1993, Nonlinear Magnetohydrodynamics (Cambridge: Cambridge Univ. Press)
Biskamp, D. 2000, Magnetic Reconnection in Plasmas (Cambridge: Cambridge Univ. Press)
Biskamp, D., & Schwarz, E. 2001, Phys. Plasmas, 8, 4729
Boozer, A. H. 1986, J. Plasma Phys., 35, 133
Che, H., Drake, J. F., & Swisdak, M. 2011, Nature, 474, 184
Daughton, W., Roytershteyn, V., Albright, B. J., et al. 2009, Phys. Rev. Lett., 103, 065004
Diamond, P. H., & Hahm, T. S. 1995, Phys. Plasmas, 2, 3640
Diamond, P. H., Hazeltine, R. D., An, Z. G., Carreras, B. A., & Hicks, H. R. 1984, Phys. Fluids, 27, 1449
Diamond, P. H., Itoh, S. I., & Itoh, K. 2010, Modern Plasma Physics: Vol. 1, Physical Kinetics of Turbulent Plasmas (Cambridge: Cambridge Univ. Press)
Diamond, P. H., Itoh, S.-I, Itoh, K., & Hahm, T. S. 2005, Plasma Phys. Control. Fusion, 47, R355
Diamond, P. H., & Malkov, M. 2003, Phys. Plasmas, 10, 2322
Drake, J. F., Kleva, R. G., & Mandt, M. E. 1994, Phys. Rev. Lett., 73, 1251
Drake, J. F., Swisdak, M., Cattell, C., et al. 2003, Science, 299, 873
Drake, J. F., Swisdak, M., Che, H., & Shay, M. A. 2006, Nature, 443, 553
Gil, L., & Sornette, D. 1996, Phys. Rev. Lett., 76, 3991
Goldreich, P., & Sridhar, S. 1995, ApJ, 438, 763
Greene, J. M. 1988, J. Geophys. Res., 93, 8583
Gruzinov, A. V., & Diamond, P. H. 1994, Phys. Rev. Lett., 72, 1651
Gurcan, O. D., Diamond, P. H., & Hahm, T. S. 2006, Phys. Plasmas, 13, 152306
Huang, Y. M., & Bhattacharjee, A. 2010, Phys. Plasmas, 17, 062104
Hwa, T., & Kardar, M. 1992, Phys. Rev. A, 45, 7002
Iroshnikov, P. S. 1964, SvA, 7, 566
Ji, H., & Daughton, W. 2011, Phys. Plasmas, 18, 111207
Kadomtsev, B. B. 1975, Sov. J. Plasma Phys., 1, 389
Kadomtsev, B. B., & Pogutse, O. P. 1979, Nucl. Fusion Suppl., 1, 649
Kim, E. J., & Diamond, P. H. 2001, ApJ, 556, 1052
Kowal, G., Lazarian, A., Vishniac, E. T., & Otmianowska-Mazur, K. 2009, ApJ, 700, 63
Kraichnan, R. H. 1965, Phys. Fluids, 8, 1385
Kulsrud, R. M. 2000, arXiv:astro-ph/0007075
Kulsrud, R. M. 2001, Earth Planets Space, 53, 417
Kulsrud, R. M. 2005, Plasma Physics for Astrophysics (Princeton, NJ: Princeton Univ. Press)
Lazarian, A., & Vishniac, E. 1999, ApJ, 517, 700
Lin, R. P., Shwartz, R. A., Kane, S. R., Pelling, R. M., & Hurley, K. C. 1984, ApJ, 283, 421
Loureiro, N. F., Schekochihin, A. A., & Cowley, S. C. 2007, Phys. Plasmas, 14, 100703
Loureiro, N. F., Uzdensky, D. A., Schekochihin, A. A., Cowley, S. C., & Yousef, T. A. 2009, MNRAS, 399, L146
Lu, E. T., & Hamilton, R. J. 1991, ApJ, 380, L89
Malyshkin, L. M., Linde, T., & Kulsrud, R. M. 2005, Phys. Plasmas, 12, 102902
Maron, J., & Goldreich, P. 2001, ApJ, 554, 1175
Matthaeus, W. H., & Lamkin, S. L. 1985, Phys. Fluids, 28, 303
Matthaeus, W. H., & Lamkin, S. L. 1986, Phys. Fluids, 29, 2513
Ng, C. S., & Ragunathan, S. 2011, in Proc. 5th Int. Conf., Numerical Modeling of Space Plasma Flows, ed. N. V. Pogorelov (San Francisco, CA: ASP), 124
Papadopoulos, K. 1977, Rev. Geophys. Space Phys., 15, 113
Parker, E. N. 1957, J. Geophys. Res., 62, 509
Parker, E. N. 1979, Cosmical Magnetic Fields (Oxford: Oxford Univ. Press)
Parker, E. N. 1988, ApJ, 330, 474
Petschek, H. E. 1964, in Physics of Solar Flares, ed. W. N. Weiss (SP-5; Greenbelt, MD: NASA), 425
Pouquet, A., Frisch, U., & Leorat, J. 1976, J. Fluid Mech., 77, 321
Priest, E. R., & Forbes, T. 2000, Magnetic Reconnection: MHD Theory and Applications (Cambridge: Cambridge Univ. Press)
Retinò, A., Sundkvist, D., Vaivads, A., et al. 2007, Nature Phys., 3, 235
Sagdeev, R. Z., & Galeev, A. A. 1969, Nonlinear Plasma Theory (New York: Benjamin)
Samtaney, R., Loureiro, N., Uzdensky, D., Schekochihin, A., & Cowley, S. 2009, Phys. Rev. Lett., 103, 105004
Shay, M. A., Drake, J. F., & Rogers, B. N. 2001, J. Geophys. Res., 106, 3759
Shibata, K., & Tanuma, S. 2001, Earth Planets Space, 53, 473
Strauss, H. R. 1976, Phys. Fluids, 19, 134
Strauss, H. R. 1986, Phys. Fluids, 29, 3668
Sweet, P. A. 1958, in IAU Symp. 6, Electromagnetic Phenomena in Cosmical Plasmas, ed. B. Lehnert (New York: Cambridge Univ. Press), 123
Syrovatskii, S. I. 1978, Sol. Phys., 58, 89
Taylor, J. B. 1974, Phys. Rev. Lett., 33, 1139
Uzdensky, D. A. 2003, ApJ, 587, 450
Uzdensky, D. A., Loureiro, N. F., & Schekochihin, A. A. 2010, Phys. Rev. Lett., 105, 235002
Wang, X. G., Ma, Z. W., & Bhattacharjee, A. 1996, Phys. Plasmas, 3, 2129
Woltjer, L. 1958, Proc. Natl Acad. Sci., USA, 44, 480
Wright, A. N., & Berger, M. A. 1989, J. Geophys. Res., 94, 1295
Yoshizawa, A. 1984, Phys. Fluids, 27, 1377
Zweibel, E. G., & Yamada, M. 2009, ARA&A, 47, 291